Running head: PbrSYP71 regulates ER accumulation in pollen tube

Corresponding author:

Peng Wang, E-mail: wangpeng@njau.edu.cn;

Juyou Wu, E-mail: juyouwu@njau.edu.cn

PbrSYP71 regulates ER accumulation by interacting with actin during pollen tube growth in *Pyrus*

Mingliang Zhang[1], Ningyi Zhang[1], Chao Tang[1], Ming Qian[1], Mengjun Sun[1], Zongqi Liu[1], Zhu Xie[1], Hao Zhang[1], Zhuqin Liu[3], Shaoling Zhang[1], Peng Wang[1]* and Juyou Wu[1,2]*

1. Sanya Institute of Nanjing Agricultural University, State Key Laboratory of Crop Genetics & Germplasm Enhancement and Utilization, Nanjing Agricultural University, Nanjing 210095, China

2. Zhongshan Biological Breeding Laboratory, No.50 Zhongling Street, Nanjing, Jiangsu 210014, China

3. Ningbo Key Laboratory of Charateristic Horticultural Crops in Quality Adjustment and Resistance Breeding, Ningbo Academy of Agricultural Science, Ningbo 315040, Zhejiang, China

*To whom correspondence should be addressed:

Peng Wang, E-mail: wangpeng@njau.edu.cn;

Juyou Wu, E-mail: juyouwu@njau.edu.cn

One-sentence summary: PbrSYP71, a syntaxin of plant protein, regulates ER accumulation by interacting with actin for pollen tube growth.

Author contributions: Juyou Wu, Mingliang Zhang, and Ming Qian designed the experiments; Mingliang Zhang, Chao Tang, and Mengjun Sun conducted the

experiments, with the help from Zongqi Liu, Zhu Xie, Hao Zhang, and Peng Wang; Mingliang Zhang, Juyou Wu, and Chao Tang wrote the manuscript; Ningyi Zhang, Peng Wang, Zhuqin Liu and Shaoling Zhang critically read and commented on the manuscript.

Funding information: This work was supported by Jiangsu Agricultural Science and Technology Innovation Fund (CX(22)3044), the National Natural Science Foundation of China (32102358), the Natural Science Foundation of Jiangsu Province (BK20210394), the Project Funded by the Priority Academic Program Development of Jiangsu Higher Education Institutions, and the Earmarked Fund for China Agriculture Research System (CARS-28).

Abstract

The pollen tube secretion system provides essential substances to support polarized pollen tube growth. The endoplasmic reticulum (ER) is a crucial component of the secretory system, and is predominantly concentrated in the pollen tube subapical region. However, the mechanism underlying the regulation of ER accumulation in pollen tube remains unclear. In this study, we identified a syntaxin protein PbrSYP71 that promoted pollen tube growth by regulating ER aggregation at pollen tube tip in pear. We found that PbrSYP71 anchored ER via the transmembrane domain. Reducing PbrSYP71 expression decreased the accumulation of ER in pollen tube. Moreover, overexpression of *PbrSYP71* resulted in bundle-like aggregation of the ER in tobacco leaf cells. Such aggregation state was disappeared when cytoplasmic domain of PbrSYP71 protein was absent or actin cytoskeleton was depolymerized. Additionally, the ER accumulation was decreased when the actin filament was depolymerized in pear pollen tube. We conclude that PbrSYP71 positively regulates ER accumulation in the subapical area of pollen tube by anchoring ER to actin, providing new insights into the underlying mechanisms of ER accumulation during polarized cell growth.

Key words

actin cytoskeleton, endoplasmic reticulum, actin filament, PbrSYP71, pear (*Pyrus bretschneideri*), pollen tube, syntaxin

Abbreviations

ER, Endoplasmic reticulum; SNARE, soluble N-ethylmaleimide-sensitive factor attachment protein receptor; F-actin, actin filaments; v-SNAREs, vesicle-associated SNAREs; t-SNAREs, target cell-associated; SYP, syntaxin of plants; s-ODN, sense oligodeoxynucleotide; as-ODN, antisense oligodeoxynucleotide; S4B, pontamine Fast Scarlet 4B; LCI, luciferase complementation imaging; Y2H, Yeast two-hybrid; CB, Cytochalasins B; TM, transmembrane; aa, amino acids

Introduction

Pollen tube delivers male gametes to the ovaries for double fertilization, which is a necessary step for sexual reproduction in flowering plants. The polarized growth of pollen tube is a very fast process, which requires essential materials supported by secretory system consisting of the endoplasmic reticulum (ER), the Golgi apparatus, and vesicles for cell wall synthesis and plasma membrane expansion within the apical region (Steer and Steer, 1989; Campanoni and Blatt, 2007; Ruan *et al*., 2020). Meanwhile, pollen tube requires intense movements of secretory system to ensure the efficient delivery of these materials to the growing tip. However these distribution and movements are not completely randomized, instead, specific classes of organelles and vesicles are aggregated at the pollen tube tip (Cai *et al*., 2015). For example, secretory vesicles and ER respectively accumulate at apical and subapical area of pollen tube (Parton *et al*., 2001; Lovy-Wheeler *et al*., 2007). Exploring the molecular mechanisms of secretion system aggregation in pollen tube is crucial for understanding its rapid polarized growth.

The ER dynamically spreads throughout the cytoplasm and is crucial for cellular health (Westrate *et al*., 2015; Zheng *et al*., 2022). ER accumulation is regulated by the actin cytoskeleton, which is further mediated by actin-linker proteins. For now, two actin-linker proteins are identified, including AtSYP73 (a syntaxin protein of plants) and NET 3B in *Arabidopsis* (Cao *et al*., 2016; Wang and Hussey, 2017). The aggregation state of the ER in non-polarized growing tissues (e.g. leaves) is formed by an increase in the actin-linker protein and is decomposed by the depolymerization of the actin cytoskeleton (Cao *et al*., 2016; Wang and Hussey, 2017). In polarized growing tissues like pollen tube, action cytoskeleton is found to regulate ER aggregation at the subapice of pollen tube (Lovy-Wheeler *et al*., 2007). The role of actin-linker proteins (i.e. AtSYP73 protein that is found to localized at ER) in regulating ER aggregation in pollen tube, however, is still unknown.

AtSYP73 is a member of the plant SYP7 subgroup of the soluble N-ethylmaleimide-sensitive factor attachment protein receptor (SNARE) proteins, which is important for membrane fusion (Jahn and Scheller, 2006). SNAREs are

divided into vesicle-associated SNAREs (v-SNAREs) and target cell-associated SNAREs (t-SNAREs) based on their subcellular localization, and are divided into R-SNARE and Q-SNARE based on their conserved residues. Q-SNARE is further classified into three types, i.e. Qa-, Qb-, and Qc-SNARE (Lipka *et al*., 2007). In general, R-SNAREs function as v-SNAREs, while Q-SNAREs act as t-SNAREs. v-SNAREs and t-SNAREs are two important components in exocytosis process. v-SNAREs are localized at vesicle, which need to be attached to "t-SNARE complex", composed of three t-SNARE proteins localized at target membrane, to form a core four-helix SNARE bundle called trans-SNARE complex to finish the membrane fusion (Jahn and Scheller, 2006; Han *et al*., 2017). For tissues (e.g. leaves) in which ER is randomly distributed, exocytosis occurs at different directions in the tissue, causing non-polarized growth of these tissues (Cao *et al*., 2016; Schwarz and Blower, 2016; Akita *et al*., 2017). In some tissues (e.g. pollen tube), ER is aggregated at their specific location (Campanoni and Blatt, 2007; Cheung and Wu, 2007; Lovy-Wheeler *et al*., 2007; Hepler and Winship, 2015), exocytosis thus potentially causes polarized growth of such tissues.

In "t-SNARE complex", one helix always comes from syntaxin group (Weimbs *et al*., 1997; Sanderfoot *et al*., 2000). Syntaxin of plants (SYP) is categorized into eight subgroups (SYP1-8) as part of the Q-SNARE complex. Within *Arabidopsis* the SYP1, 2, 3, 4, and 8 subgroups are associated with Qa-SNARE, while the SYP5, 6, and 7 subgroups are linked to Qc-SNARE (Sanderfoot *et al*., 2000; Lipka *et al*., 2007). In SYP7 subgroup in *Arabidopsis*, AtSYP73 regulates the ER accumulation and movement by interacting with actin in hypocotyl epidermal cells (Cao *et al*., 2016). It remains unclear whether the members of the SYP7 subgroup play a role in the ER distribution in the pollen tube.

Pear (*Pyrus bretschneideri*) is an important orchard crop worldwide, of which the pollination is a very laborious but necessary process due to its self-incompatibility. Breeding self-compatibility cultivars has always been an important goal in pear production, for which understanding the underlying mechanisms of pollen tube growth is very relevant. Here, we chose pear (*Pyrus bretschneideri* cv. 'Dangshansuli')

as the case study due to its well-documented genome information that provides fundamental database for studying the molecular mechanisms of pollen tube growth (Wu *et al*., 2013). We identified a gene from the SYP7 subgroup, *PbrSYP71*, which was highly expressed in pear pollen and promotes pollen tube growth. We found that the PbrSYP71 protein was anchored to the ER, regulating the accumulation of ER in the pear pollen tube. Moreover, the accumulation of PbrSYP71 was dependent on actin cytoskeleton. Meanwhile, the aggregation of ER in pear pollen tube required the support of F-actin. These results indicate that PbrSYP71 serves as a bridge connecting ER and F-actin, anchors ER to F-actin to maintain the accumulation of ER in the subapical area, thereby promoting efficient and rapid transport of materials to the rapidly growing tip of the pollen tube.

Results

PbrSYP genes were identified in pear and *PbrSYP71* was specifically expressed in the pollen tube

A total of 43 *SYP* members from the pear genome were identified (Table S1). These proteins were distributed in 8 subgroups (SYP1-SYP8) based on evolutionary relationships (Figure S1). The SYP7 subgroup included five members, i.e. *PbrSYP71*, *72*, *73*, *74*, and *75*, which had high level of homology and conservative domain and motif with *AtSYP71*, *72*, and *73* (Figure 1A, B; Figure S2, and Figure S3). Our RT-qPCR data showed that among all five PbrSYPs, only *PbrSYP71*, *73* and *75* were expressed in the pollen (in grains and tubes), with PbrSYP71 showing the highest expression level (Figure 1C). Expressions of PbrSYP72 and 74 were hardly detected in the pollen. Moreover, *PbrSYP71* was only highly expressed in the pollen but not in any other tissues e.g. leaves or stems (Figure S4, and Figure S5). These suggested an important role of *PbrSYP71* in pear pollen tube growth.

PbrSYP71 positively regulated pear pollen tube growth

To verify the function of *PbrSYP71* in pear pollen tube growth, the *PbrSYP71* expression was knocked down using as-ODN silencing technology. The phenotype of pear pollen tubes was mal-functioning when treated with as-ODN-PbrSYP71 (Figure 2A). The relative expression of *PbrSYP71* in pollen tube treated with

as-ODN-PbrSYP71 reduced remarkably compared with that in s-ODN treated pollen tube (Figure 2B). The germination rate of pollen grains was decreased when inhibiting the expression of *PbrSYP71* (Figure 2C). The pollen tube length was significantly decreased whereas pollen tube diameter was increased in the presence of as-ODN-PbrSYP71 (Figure 2A, D, E). The cellulose content of the pollen tube was significantly decreased when the *PbrSYP71* expression was knocked down (Figure 2F-H). These results suggested that knockdown of *PbrSYP71* expression caused pollen tube defects in terms of pollen size growth and cellulose biosynthesis.

PbrSYP71 protein was localized at ER

The subcellular localization of PbrSYP71 assays were performed in leaf of *N. benthamiana.* We found that PbrSYP71-GFP localized to cytoplasm and perinuclear area (Figure 3 A, C, and D), in which perinuclear area was composed of ER (Schwarz and Blower, 2016). Then, the PbrSYP71-GFP fusion protein and a ER marker, AtRTP1-mCherry (Pan *et al*., 2016), were co-expressed in leaf epidermal cells. Results showed that their fluorescence patterns overlapped (Figure 3E), suggesting that PbrSYP71 was localized to ER. To further verify whether the transmembrane (TM) domain of the PbrSYP71 protein anchors the ER, we constructed a PbrSYP71-TM-GFP vector containing the TM domain (236-265 aa) (Figure S6A; Table S2). When the PbrSYP71-TM-GFP fusion protein and AtRTP1-mCherry were co-expressed in leaf epidermal cells, the co-localization of PbrSYP71-TM-GFP and AtRTP1-mCherry was observed (Figure S6B). These results indicated that PbrSYP71 localized to the ER via TM domain.

***PbrSYP71* regulated ER distribution in pear pollen tube**

ER and secretory vesicles labeling results in pear showed that the ER accumulated at the pollen tube sub-apical area and vesicles accumulated at the pollen tube tip, forming a V-shaped tip followed by a tail (Figure S7). Similar results were also found in lily pollen tube (Parton *et al*., 2001; Lovy-Wheeler *et al*., 2007; Hepler and Winship, 2015). The fluorescence intensity of the ER at sub-apical area (area of black box) significantly increased (Figure 4A and C) and the apical accumulation of vesicles was disrupted when treating pollen tube with as-ODN-PbrSYP71 (Figure 4B, D and

E). These results suggested that *PbrSYP71* positively regulated accumulations of ER and vesicles in pear pollen tube.

The accumulation and movement of PbrSYP71 protein was dependent on actin cytoskeleton

PbrSYP71 protein was predicted to contain an actin-binding domain (ABD), a SNARE-Qc domain and a TM domain (Figure 5A). Based on protein sequence alignment, the ABD domain of PbrSYP71 was highly conserved with ABD domain (77-95 aa) of the AtSYP73 protein (Figure 5B). Such a structure indicated that PbrSYP71 was able to bind to actin. To further confirm this interaction, we chose actin protein PbrActin1 (Pbr032870.1) as a candidate of PbrSYP71 interacting protein. Y2H assays revealed that the yeast cells co-expressing PbrSYP71-BD and PbrActin1-AD were able to grow on medium lacking Leu, Trp, Ade, and His (Figure 5C). In the LCI assays, fluorescence was observed when PbrSYP71-cLUC and PbrAtin1-nLUC were co-expressed in tobacco leaves, as well as when PbrSYP71-ABD-cLUC and PbrAtin1-nLUC were co-expressed; however, no fluorescence was observed in the controls in both cases (Figure 5D, E). These results suggested that PbrSYP71 interacted with PbrActin1 by ABD domain.

To test the function of actin cytoskeleton on the accumulation of PbrSYP71 protein, we examined the subcellular localization of PbrSYP71, TM domain of PbrSYP71 (PbrSYP71-TM), and Cytoplasmic domain of PbrSYP71 (PbrSYP71-N) in tobacco leaf cells (Figure 6A). PbrSYP71-GFP distributed around the whole cytoplasm and presented bundle structure (Figure 6B). When actin cytoskeleton was depolymerized with the actin cytoskeleton depolymerizing agent Cytochalasins B (CB), PbrSYP71-GFP also distributed in the whole cytoplasm, but presented cisternae network structure that was consistent with the structure of the ER (Figure 6C) (Brandizzi *et al*., 2002). These results suggested that the shape of PbrSYP71 depended on actin cytoskeleton. Further, we observed that PbrSYP71-TM-GFP distributed in the whole cytoplasm presenting cisternae network structure (Figure 6D). Cisternae network structure of PbrSYP71-TM-GFP enlarged when treated with CB (Figure 6E), which was similar to PbrSYP71-GFP treated with CB (Figure 6C).

PbrSYP71-N-GFP also distributed in the whole cytoplasm, but presented a more obvious bundle structure than that of PbrSYP71-GFP (Figure 6F). When PbrSYP71-N-GFP was treated with CB, the bundle structure transitioned into circular structure that evenly distributed in the cytoplasm (Figure 6G). These results suggested that the state of aggregation of PbrSYP71 depended on cytoplasmic domain and actin cytoskeleton. PbrSYP71 and PbrSYP71-TM were located at ER, and their cisternae network structures were consistent with the ER structure. Thus, the aggregation state of the ER was confirmed to be regulated by PbrSYP71 protein interaction with actin.

The bundles of PbrSYP71-GFP were continuously moving and changing in tobacco leaf cells (Movie S1). When the actin cytoskeleton was depolymerized, the movement of PbrSYP71-GFP was reduced with bundles disappearing (Movie S2). PbrSYP71-TM-GFP, presenting cisternae network, also kept moving (Movie S3), and the movement was reduced when treated with CB (Movie S4). We found that the PbrSYP71-N-GFP presented strong bundles and exhibited rapid movements (Movie S5), and the movement ceased when actin cytoskeleton was depolymerized (Movie S6).

F-actin maintained ER distribution for pollen tube growth

To verify the function of F-actin on ER accumulation and vesicle accumulation, the F-actin was depolymerized by treatment with CB in pear pollen tube. The ER accumulation disappeared in the sub-apical region and uniformly distributed throughout the cytoplasm when pollen tube was treated with CB (Figure 7A and C). The apical accumulation of vesicles was reduced as well (Figure 7B, D and E). pollen tube evolved abnormal phenotypes including decreased germination rate (Figure 8B), reduced length (Figure 8A and C), increased diameter (Figure 8A and D) and decreased cellulose content of cell wall (Figure 8E, F and G). These results suggested that F-actin maintained the ER and vesicles accumulations, and supported pollen tube growth.

Discussion

Syntaxin protein PbrSYP71 regulates cell tip growth

Syntaxin proteins are required for eukaryotes development as they play key roles in

cell tip growth (Hong *et al*., 2010; Qi *et al*., 2016). Here, we identified a syntaxin protein – PbrSYP71 – that was involved in pear pollen tube tip growth by regulating accumulations of the ER and secretory vesicles, and cell wall cellulose biosynthesis (Figure 2; Figure 4). Previously, syntaxin proteins are found to regulate cell tip growth in bacteria, fungi and model plant species *Arabidopsis*. For examples, in yeast, syntaxin Tlg1p protein mediates polarized growth by mediating delivery of chitin synthase III (Holthuis *et al*., 1998); in *N. crassa*, syntaxin NSYN1/2 proteins are involved in hyphal tip growth by regulating vesicle fusion (Gupta *et al*., 2003); in *Arabidopsis*, syntaxin of plant SYP121, SYP123, SYP132, and AtSYP81 proteins promote root tip growth by mediating vesicle fusion (Hirano *et al*., 2023; Wang *et al*., 2023), SYP124 is involved in pollen tube tip growth (Silva *et al*., 2010), SYP1s and SYP72 plays a key role in pollen development and germination (Li *et al*., 2019; Zhou *et al*., 2022). To our knowledge, we are the first to identify the role of syntaxin protein in polarized cell growth in important crop plants (i.e. pear). All together, these results suggest that the function of syntaxin proteins in regulating cell tip growth is conserved across different species.

PbrSYP71 regulates cell tip growth by affecting ER accumulation and membrane fusion

We showed that PbrSYP71 protein promoted the ER accumulation in pear pollen tube (Figure 4), which was necessary for pollen tube growth (Figure 2). Recent studies have found that the distribution of ER is directly related to cell health and cell polarity. For examples, in human U2OS cells, when ER distribution is disrupted, the distribution of other organelles is also affected, resulting in neurologic disorders and cancer (Zheng *et al*., 2022). ER accumulation at the root hair tip is necessary for the root hair development (Campanoni and Blatt, 2007). In addition, PbrSYP71 protein, as t-SNARE protein, was localized at ER (Figure 3). Previously, syntaxin proteins are found to mediate vesicle fusion in together with ER. For example, ER-located t-SNARE proteins (i.e. syntaxin 18) mediate the fusion of COPI (coatomer complex I) vesicles, deriving by Golgi with ER and the fusion of legionella-containing vacuole with ER (Spang and Schekman, 1998; Hatsuzawa *et al*., 2006; Spang, 2013;

Kawabata *et al*., 2021). Therefore, we propose that PbrSYP71 protein located at ER could mediate the fusion of vesicles with ER for maintaining the functioning of secretory system in pear pollen tube. Previous studies on the function of syntaxin in cell polar growth mainly focus on regulating the fusion of vesicles and plasma membranes. For examples, syntaxin proteins located in plasma membrane, including syntaxin Tlg1p (in yeast), syntaxin NSYN1/2 (in *N. crassa*), SYP121 SYP123, SYP124, and SYP132 (in *Arabidopsis*), are involved in regulating the membrane fusion of secretory vesicle with plasma membrane for cell tip growth (Holthuis *et al*., 1998; Gupta *et al*., 2003; Silva *et al*., 2010; Hirano *et al*., 2023). Here, we showed that PbrSYP71 was located at ER and positively regulate vesicle secretion, which provided a specific target for studying the function of syntaxin in mediating vesicle fusion with ER during pollen tube growth. We conclude that syntaxin proteins regulates ER accumulation in addition to mediating membrane fusion in cell polar growth.

The cytoplasmic domain of PbrSYP71 protein regulates the ER accumulation and movement

We found that the ER accumulation in pear pollen tube depended on the interaction between cytoplasmic domain of PbrSYP71 protein and actin (Figure 5; Figure 6; Figure 7). Similar functions of syntaxin proteins exist in leaf tissues and animal cells. For examples, in *Arabidopsis*, cytoplasmic domain of AtSYP73 protein interacts with actin, leading to the ER accumulation (Cao *et al*., 2016). In INS-1 and CHO cells, H_{abc} domains of syntaxin 1A determine its cluster distribution without affecting its localization on plasma membrane (Yang *et al*., 2006; Fan *et al*., 2007). These results showed that cytoplasmic domain of syntaxin plays a key role in ER accumulation. Interestingly, we found that cytoplasmic domain of PbrSYP71 moved on the actin cytoskeleton independent of ER movement (Movie S1-6), suggesting that the ER movement may be driven by the movement of PbrSYP71 cytoplasmic domain. In *Arabidopsis*, AtSYP73 protein has been found to regulate the ER flow rate (Cao *et al*., 2016). Our results clarified the role of PbrSYP71 cytoplasmic domain in regulating ER accumulation and movement, further broadening our understanding of the

functions of syntaxin proteins in exocytosis process during cellular polar growth.

The intracellular localization of PbrSYP71 protein is dependent on TM domain

Different syntaxin proteins have different subcellular localizations. For examples, syntaxin 1 and SYP131 (in mammals and *Arabidopsis*) are located on plasma membrane (Teng *et al*., 2001; Ichikawa *et al*., 2015); syntaxin 5 and SYP31 (in mammals and *Arabidopsis*) are presenting on the Golgi apparatus (Teng *et al*., 2001; Rui *et al*., 2021); syntaxin 18 and SYP73 (in mammals and *Arabidopsis*), as well as PbrSYP71 in pear found in our study, are located at ER (Figure 3) (Teng *et al*., 2001; Cao *et al*., 2016). The domains of syntaxin proteins that determine their specific subcellular localizations are also different for different syntaxin members (Kasai and Akagawa, 2001). We found that PbrSYP71 anchored the ER via TM domain (Figure S6). Additionally, the length of the TM domain determines the subcellular localization of syntaxins 3 (Watson and Pessin, 2001). The trans-Golgi network localization of syntaxin 6 depends on H2 domain and YGRL motif (Watson and Pessin, 2000), and the Golgi localization of syntaxin Sed5p relies on its the TMD amino acid, the COPI coatomer binding motif, and the folded-back conformation (Gao and Banfield, 2020). Thus, the conserved structures that influence the syntaxin subcellular localization differ between syntaxin proteins.

Conclusion

We presented a model describing the regulatory role of PbrSYP71 in ER accumulation at the pollen tube subapical area, taking an important horticultural crop pear as an example (Figure 9). PbrSYP71 protein anchors the ER via the TM domain and bridges ER with F-actin through actin-binding domain (ABD) interaction. This maintains ER accumulation at the subapical region of pollen tube, providing materials for pollen tube growth. Insufficient PbrSYP71 protein, however, lead to the loss of connection between ER and F-actin, resulting in no ER aggregation and evenly ER distribution. Consequently, the reduction in secretory vesicles fails to provide sufficient materials for pollen tube growth, causing abnormal pollen tube phenotypes. The absence of track and collar structures for PbrSYP71 protein attachment, following F-actin depolymerization, reduce ER accumulation and secretory vesicle

content. In conclusion, we elucidate the key role of *PbrSYP71* in the ER accumulation during pollen tube growth, providing new insights for the role of syntaxin proteins in exocytosis process during polarized cell growth.

Materials and methods

Plant materials

Pear trees (*P. bretschneideri* cv. "Dangshansuli") were grown in the Fruit Experimental Field of Nanjing Agricultural University, Nanjing, China (32°N, 118°E). Mature pollens from these trees were collected and stored at -20°C in a desiccator for later use.

Identification and basic information analysis of *SYP* genes in pear

Protein sequences of 25 AtSYP were acquired from the TAIR (https://www.arabidopsis.org/) and these sequences were used as queries to perform BLASTP searches against the Pear Genome Database (http://pcwgdb.njau.edu.cn/) (Hu *et al*., 2023) by TBtools software (China) with an e-value cut-off of $1.0 \times e^{-5}$ (Chen *et al*., 2023). Meanwhile, hidden Markov model profiles of the SYP domain (PF05739) were submitted to HMMsearch software to search for candidate SYP proteins in pear (Johnson *et al*., 2010). Redundant sequences from all obtained gene sequences were removed. SMART (http://smart.embl-heidelberg.de/) and the Pfam database (http://pfam.xfam.org/) were applied to detect SNARE functional domains in obtained sequences (Letunic *et al*., 2021; Mistry *et al*., 2021). The relative molecular weights and isoelectric points of PbrSYP proteins were determined by ExPASY (http://web.expasy.org/compute_pi/) (Artimo *et al*., 2012). The transmembrane structure and motifs of PbrSYP proteins were respectively predicted using CCTOP (https://cctop.ttk.hu/) (Dobson *et al*., 2015) and MEME (https://meme-suite.org/meme/) (Bailey *et al*., 2015). Actin-binding domain (ABD) LIG_Actin_WH2_2 was predicted by the Eukaryotic Linear Motif (ELM) program (Dinkel *et al*., 2016).

Phylogenetic analysis

Phylogenetic analysis of 43 pear *SYP* members was performed by MEGA7.0 software (Kumar *et al*., 2016). Evolutionary analysis was conducted using 43 sequences of pear

SYP proteins and 25 sequences of *Arabidopsis* SYP proteins. ClusterW alignment of all sequences was preferred, followed by the construction of a *SYP* evolutionary tree using the Neighbor Joining, with internal branches being taken 1000 times. Phylogenetic relationships of pear and *Arabidopsis* SYP7 subgroup proteins were conducted using the Neighbor Joining method in MEGA7.

Pollen culture *in vitro*

The method of cultivating pollen *in vitro* can be found in our previous study (Tang *et al*., 2023). Mature pollen was taken out from -20°C and slowly thawed to room temperature, and evenly dispersed in a pollen medium (containing 0.5 mM calcium nitrate $Ca(NO_3)_2$, 1.5 mM boric acid (H_3BO_3), 25 mM 2-(N-morpholino) ethanesulfonic acid hydrate (MES) and 450 mM sucrose (sucrose) with pH 5.8, and cultured at 25°C/120 rpm. Then, the pollen tubes were collected by centrifugation at 2,000 rpm for 5 min, and then stored at -80°C.

RNA extraction

Total RNA was extracted using a FastPure® Universal Plant Total RNA Isolation Kit (Vazyme, China). The HiScript® II1st Strand cDNA Synthesis Kit (Vazyme, China) was employed for reverse transcribing the RNA into cDNA.

Quantitative real-time PCR (RT-qPCR) assays

The quantitative specific primers of *SYP* gene family members in pear were designed by the online Primer BLAST tool (https://www.ncbi.nlm.nih.gov/tools/primer-blast/) (Ye *et al*., 2012). LC480 II light cycler (Roche, Germany) instrument was used for qRT-PCR. The volume of each sample was 20 μL, which included 5 μL of specific primers with a concentration of 10 μM, 2 μL of cDNA with a concentration of 100ng/μL, 3 μL of ddH_2O, and 10 μL of 2 × SYBR mixed dye (Vazyme, China). The reaction procedure for qPCR followed three steps, being that step 1 is incubating at 95℃ for 5 minutes, step 2 is incubating at 95 ℃ for 3 seconds, followed by 60 ℃ for 10 seconds and 72 ℃ for 10 seconds, for a total of 45 cycles, and step 3 is drawing a dissolution curve to verify primer specificity. These data were analyzed using LightCycler480 software. *PbrUBQ* (Pbr035452.1) was used as an internal reference in pear pollen tube to normalize the expression levels of *SYP* genes. The relative

expression level of *SYP* was calculated according to the $2^{-\Delta\Delta Ct}$ method. The primers of qRT-PCR assays were shown in Supplemental Table S3.

Analysis of *PbrSYP* genes expression based on transcriptome data

The expression levels of *PbrSYP* genes were analyzed based on our previous transcriptomic data (http://pcwgdb.njau.edu.cn/) (Zhou *et al*., 2016; Hu *et al*., 2023) in 19 pear tissues including four seedling tissues (JSM, juvenile stem; CT, cotyledon; JLF, juvenile leaf; and RT, root), six flower organ tissues (OA, ovary; SP, sepal; ST, stamen; SY, style; PT, petal; and FLS, flower stalk), five fruit tissues (FTC, fruit core; FS, flesh ;FTS, fruit stalk; SD, seed; and PR, pericarp), flower bud (FLB), stem (SM), adult leaf (ALF), leaf bud (LFB). The transcripts per kilobase million (TPM) values were used for measuring the *PbrSYP* gene expression level at different developmental stages during pollen germination and pollen tube growth (MP, mature pollen grains; HP, hydrated pollen grains; PT, growing pollen tubes; and SPT, stopped-growth pollen tubes). The RPKM (reads per kilobase per million) values were used for measuring the gene expression level. These data of expression levels of *PbrSYP* genes were given in Supplemental Table S4 and Table S5.

Antisense oligodeoxynucleotide (as-ODN) assays

Antisense oligodeoxynucleotides (ODN) assays were performed as described previously in reference to the previous study (Chen *et al*., 2018). First, the mixture of ODN sequence and Lipofectamine 3000 (Thermo Fisher, USA) transfection reagent was incubated at room temperature for 15 minutes. Then the mixture was added to the pollen tube culture medium. The final concentration of ODN was 40 μM. Pollen was cultured for 3 h with 25℃ and 120 rpm. The images of pollen germination and pollen tube growth were obtained using an optical microscope, and the diameter and length of pollen tubes were measured using ImageJ software (https://imagej.nih.gov/ij/). The as-ODN Primer of PbrSYP71 gene was designed using online RNA fold website Server (http://rna.tbi.univie.ac.at//cgi-bin/RNAWebSuite/RNAfold.cgi). The primers of ODN were shown in Supplemental Table S3.

Detection of cellulose in pollen tube cell wall

Cellulose staining of pollen tube cell wall was conducted based on our previous study

(Li *et al*., 2022). First, prepared pollen tubes were washed with phosphate buffered saline (PBS) three times, and then fixed with 4% paraformaldehyde for 30 minutes. After fixation, pollen tubes were transferred to PBS containing 0.01% Pontamine Fast Scarlet 4B (S4B) (Sigma-Aldrich, USA), then incubated at room temperature for 5 minutes and washed with PBS three times. The dyed pollen tube was observed using a confocal microscope LSM800 (Zeiss, Germany). The fluorescence was measured using ZEN 3.1 software (Zeiss, Germany).

Subcellular localization assays

The subcellular localization assays were performed based on (Sparkes *et al*., 2006). Firstly, the CDS of *PbrSYP71*, *PbrSYP71-TM* (amino acid residue 236-265aa), and *PbrSYP71-N* (amino acid residue 1-235aa) without stop codon were cloned into the pCAMBIA1300-35S::GFP vector to construct 35S::PbrSYP71-GFP, 35S::PbrSYP71-TM-GFP and 35S::PbrSYP71-N-GFP vectors. The CDS of AtRTP1 without stop codon was cloned into the pCAMBIA1300-35S::mCherry vector to construct 35S::AtRTP1-mCherry vector. Then, vectors were transformed into epidermal cells of *N. benthamiana*. Meanwhile, the pCAMBIA1300-35S::GFP vector was used as the control. Nucleus was marked by DAPI dye. Finally, the fluorescence was observed using an LSM800 laser scanning confocal microscope (Zeiss, Germany). The primers of subcellular localization assays were shown in Supplemental Table S3.

ER labeling

ER-Tracker Red (Beyotime, shanghai, China) – a specific red fluorescent probe for ER – was used as a marker of the ER of eukaryotic cells (Wang *et al*., 2017; Su *et al*., 2021). ER of the pollen tube was labeled ER-Tracker Red as follows: pollen tubes were transferred to pollen culture medium containing 20 μM ER-Tracker Red and allowed to incubate for 30 min. The fluorescence of ER-Tracker Red was observed using an LSM800 laser scanning confocal microscope (Zeiss, Germany).

Secretory vesicles labeling

Parton's method was used to measure secretory vesicles (Parton *et al*., 2001). The pollen tubes were transferred to pollen culture medium containing 8 μM FM4-64 and allowed to incubate for 15 min. The fluorescence of FM4-64 was observed using an

LSM800 laser scanning confocal microscope (Zeiss, Germany).

Yeast two-hybrid (Y2H) assay

The *PbrSYP71* and *PbrActin1* CDS sequences without stop codon were cloned into the pGBDT7 and pGADT7 vector to construct the PbrSYP71-BD vector and the PbrSYP71-AD vector, respectively. Then, different combinations were transferred into Y2HGold yeast cells. Finally, these yeast cells grew on selective medium lacking Leu, Trp, Ade, and His (−L/−T/−A/−H) to detect possible interactions. Growth in the medium lacking Leu, Trp, Ade, and His indicated protein-protein interactions. The AD-T and BD-lam combination was used as a negative control, and the AD-T and BD-53 combination was used as a positive control. The primers of yeast two-hybrid assays were shown in Supplemental Table S3.

Luciferase complementation imaging (LCI) assays

Firstly, The *PbrActin1* CDS without stop codon was cloned into the pCAMBIA1300-nLuc to construct PbrActin1-nLuc nLuc. The *PbrSYP71* and *PbrSYP71-ABD* (amino acid residue 77-95 aa) CDS without stop codon was cloned into the pCAMBIA1300-cLuc to construct PbrSYP71-cLuc and PbrSYP71-ABD-cLuc, respectively. Then, different combinations were transformed into leaf cells of *N. benthamiana.* Finally, the LUC activity in leaves of *N. benthamiana* was detected using In Vivo Plant Imaging System (PIXIS 1024B, Princeton Instrument, USA). The primers of LCI assays were shown in Supplemental Table S3.

Movie production

The video of PbrSYP71-GFP movement was produced using the following method. First, at least 35 consecutive fluorescence images were obtained using LSM800 laser scanning confocal microscope (Zeiss, Germany), in which fluorescence images were obtained every 14 s. Then, these images were played in chronological order (Frame Per Second=5) using ZEN 2012 software (Zeiss, Germany).

Statistical analysis

GraphPad Prism 8.2.1 (GraphPad Software, USA) was used to plot the results including their averages and the corresponding standard deviation. SPSS v22 (IBM,

USA) was used to determine statistical significance. Significant statistical differences for two samples were analyzed using the Student's *t*-test ($P < 0.01$). Significant statistically differences for multiple samples were analyzed using Duncan LSD test of one-way ANOVA ($P < 0.05$).

Supplementary data

The following supplemental materials are available:

Fig. S1 Neighbor-Joining phylogeny of SYP family proteins from *Pyrus* and *Arabidopsis*.

Fig. S2 Conservative domains analysis of proteins of SYP7 subgroup.

Fig. S3 Conserved motif analysis of SYP proteins

Fig. S4 Expression patterns of *PbrSYP* genes in different tissues of pear.

Fig. S5 The expression of *PbrSYP* genes during four development stages of pear pollen.

Fig. S6 Intracellular localization of PbrSYP71-TM to the ER in tobacco leaf cells.

Fig. S7 The distribution of ER and vesicle in pear pollen tube.

Table S1 Detailed information on *SYP* gene family members in pear.

Table S2 The 1D structure of PbrSYP proteins.

Table S3 Primers used in this study

Table S4 Expression patterns of PbrSYP genes in different tissues of pear.

Table S5 The expression of PbrSYP genes during four development stages of pear pollen.

Movie S1 The movement of PbrSYP71-GFP in tobacco leaf cells.

Movie S2 The movement of PbrSYP71-GFP treated with the actin depolymerizing agent Cytochalasins B (CB) in tobacco leaf cells .

Movie S3 The movement of PbrSYP71-TM-GFP in tobacco leaf cells.

Movie S4 The movement of PbrSYP71-TM-GFP treated with the CB in tobacco leaf cells.

Movie S5 The movement of PbrSYP71-N-GFP in tobacco leaf cells.

Movie S6 The movement of PbrSYP71-N-GFP treated with the CB in tobacco leaf cells.

Acknowledgements

We thank Dr. Yuehua Ma from Central laboratory of College of Horticulture in Nanjing Agricultural University for her technical assistance in the use of laser confocal microscopy LSM800 (Zeiss, Germany).

Conflict of interest

The authors declare no competing interests.

References

Akita K, Kobayashi M, Sato M, Kutsuna N, Ueda T, Toyooka K, Nagata N, Hasezawa S, Higaki T. Cell wall accumulation of fluorescent proteins derived from a trans-Golgi cisternal membrane marker and paramural bodies in interdigitated *Arabidopsis* leaf epidermal cells. Protoplasma. 2017:**254:**1367-377. https://doi.org/10.1007/s00709-016-0955-1

Artimo P, Jonnalagedda M, Arnold K, Baratin D, Csardi G, de Castro E, Duvaud S, Flegel V, Fortier A, Gasteiger E, et al. ExPASy: SIB bioinformatics resource portal. Nucleic Acids Res. 2012:**40:**W597-603. https://doi.org/10.1093/nar/gks400

Bailey T, Johnson J, Grant C, Noble W. The MEME Suite. Nucleic Acids Res. 2015:**43:**W39-49. https://doi.org/10.1093/nar/gkv416

Brandizzi F, Snapp E, Roberts A, Lippincott-Schwartz J, Hawes C. Membrane protein transport between the endoplasmic reticulum and the Golgi in tobacco leaves is energy dependent but cytoskeleton independent: evidence from selective photobleaching. Plant Cell. 2002:**14:**1293-1309. https://doi.org/10.1105/tpc.001586

Cai G, Parrotta L, Cresti M. Organelle trafficking, the cytoskeleton, and pollen tube growth. J Integr Plant Biol. 2015:**57:**63-78. https://doi.org/10.1111/jipb.12289

Campanoni P, Blatt M. Membrane trafficking and polar growth in root hairs and pollen tubes. J Exp Bot. 2007:**58:**65-74. https://doi.org/10.1093/jxb/erl059

Cao P, Renna L, Stefano G, Brandizzi F. SYP73 Anchors the ER to the Actin Cytoskeleton for Maintenance of ER Integrity and Streaming in *Arabidopsis*. Curr Biol. 2016:**26:**3245-3254. https://doi.org/10.1016/j.cub.2016.10.024

Chen C, Wu Y, Li J, Wang X, Zeng Z, Xu J, Liu Y, Feng J, Chen H, He Y, et al. TBtools-II: A "one for all, all for one" bioinformatics platform for biological big-data mining. Mol Plant. 2023:**16:**1733-1742. https://doi.org/10.1016/j.molp.2023.09.010

Chen J, Wang P, de Graaf B, Zhang H, Jiao H, Tang C, Zhang S, Wu J. Phosphatidic Acid Counteracts S-RNase Signaling in Pollen by Stabilizing the Actin Cytoskeleton. Plant Cell. 2018:**30:**1023-1039. https://doi.org/10.1105/tpc.18.00021

Cheung A, Wu H. Structural and functional compartmentalization in pollen tubes. J Exp Bot. 2007: **58:** 75-82. https://doi.org/10.1093/jxb/erl122

Dinkel H, Van Roey K, Michael S, Kumar M, Uyar B, Altenberg B, Milchevskaya V, Schneider M, Kühn H, Behrendt A, et al. ELM 2016--data update and new functionality of the eukaryotic linear motif resource. Nucleic Acids Res. 2016:**44:**D294-300. https://doi.org/10.1093/nar/gkv1291

Dobson L, Reményi I, Tusnády G. CCTOP: a Consensus Constrained TOPology prediction web server. Nucleic Acids Res. 2015:**43:**W408-412. https://doi.org/10.1093/nar/gkv451

Fan J, Yang X, Lu J, Chen L, Xu P. Role of H(abc) domain in membrane trafficking and targeting of syntaxin 1A. Biochem Biophys Res Commun. 2007:**359:** 245-250. https://doi.org/10.1016/j.bbrc.2007.05.065

Gao G, Banfield D. Multiple features within the syntaxin Sed5p mediate its Golgi localization. Traffic. 2020**21:**274-296. https://doi.org/10.1111/tra.12720

Gupta G, Free S, Levina N, Keränen S, Heath I. Two divergent plasma membrane syntaxin-like SNAREs, nsyn1 and nsyn2, contribute to hyphal tip growth and other developmental processes in Neurospora crassa. Fungal Genet Biol. 2003:**40:**271-286. https://doi.org/10.1016/s1087-1845(03)00109-9

Han J, Pluhackova K, Böckmann R. The Multifaceted Role of SNARE Proteins in Membrane Fusion. Front Physiol. 2017:**8:**5. https://doi.org/10.3389/fphys.2017.00005

Hatsuzawa K, Tamura T, Hashimoto H, Hashimoto H, Yokoya S, Miura M, Nagaya H, Wada I. Involvement of syntaxin 18, an endoplasmic reticulum (ER)-localized SNARE protein, in ER-mediated phagocytosis. Mol Biol Cell. 2006:**17:** 3964-3977. https://doi.org/10.1091/mbc.e05-12-1174

Hepler P, Winship L. The pollen tube clear zone: clues to the mechanism of polarized growth. J Integr Plant Biol. 2015:**57:** 79-92. https://doi.org/10.1111/jipb.12315

Hirano T, Ebine K, Ueda T, Higaki T, Watanabe-Nakayama T, Konno H, Takigawa-Imamura H, Sato M. The SYP123-VAMP727 SNARE complex delivers secondary cell wall components for root hair shank hardening in *Arabidopsis*. Plant Cell. 2023:30;35(12)**:**4347-4365. https://doi.org/10.1093/plcell/koad240

Holthuis J, Nichols B, Pelham H. The syntaxin Tlg1p mediates trafficking of chitin synthase III to polarized growth sites in yeast. Mol Biol Cell. 1998:**9:** 3383-3397. https://doi.org/10.1091/mbc.9.12.3383

Hong SY, So J, Lee J, Min K, Son H, Park C, Yun SH, Lee YW. Functional analyses of two syntaxin-like SNARE genes, GzSYN1 and GzSYN2, in the ascomycete Gibberella zeae. Fungal Genet Biol. 2010:**47:** 364-372. https://doi.org/10.1016/j.fgb.2010.01.005

Hu J, Huang B, Yin H, Qi K, Jia Y, Xie Z, Gao Y, Li H, Li Q, Wang Z, et al. PearMODB: a multiomics database for pear (*Pyrus*) genomics, genetics and breeding study. Database (Oxford). **2023:**baad050. https://doi.org/10.1093/database/baad050

Ichikawa M, Iwano M, Sato M. Nuclear membrane localization during pollen development and apex-focused polarity establishment of SYP124/125 during pollen germination in Arabidopsis thaliana. Plant Reprod. 2015:**28:** 143-151. https://doi.org/10.1007/s00497-015-0265-3

Jahn R, Scheller R. SNAREs--engines for membrane fusion. Nature reviews. Nat Rev Mol Cell Biol. 2006:**7:** 631-643. https://doi.org/10.1038/nrm2002

Johnson L, Eddy S, Portugaly E. Hidden Markov model speed heuristic and iterative HMM search procedure. BMC Bioinformatics. 2010:**11:** 431.https://doi.org/10.1186/1471-2105-11-431

Kasai K, Akagawa K. Roles of the cytoplasmic and transmembrane domains of syntaxins in intracellular localization and trafficking. J Cell Sci. 2001:**114:** 3115-3124. https://doi.org/10.1242/jcs.114.17.3115

Kawabata M, Matsuo H, Koito T, Murata M, Kubori T, Nagai H, Tagaya M, Arasaki K. Legionella hijacks the host Golgi-to-ER retrograde pathway for the association of Legionella-containing vacuole with the ER. PLoS Pathog. 2021:**17:** e1009437. https://doi.org/10.1371/journal.ppat.1009437

Kumar S, Stecher G, Tamura K. MEGA7: Molecular Evolutionary Genetics Analysis Version 7.0 for Bigger Datasets. Mol Biol Evol. 2016:**33:** 1870-1874. https://doi.org/10.1093/molbev/msw054

Li B, Li Y, Liu F, Tan X, Rui Q, Tong Y, Qiao L, Gao R, Li G, et al. Overexpressed Tomosyn Binds Syntaxins and Blocks Secretion during Pollen Development. Plant Physiol. 2019:**181:**1114-1126. https://doi.org/10.1104/pp.19.00965

Letunic I, Khedkar S, Bork P. SMART: recent updates, new developments and status in 2020. Nucleic Acids Res. 2021:**49:** D458-D460. https://doi.org/10.1093/nar/gkaa937

Li X, Tang C, Li X, Zhu X, Cai Y, Wang P, Zhang S, Wu J. Cellulose accumulation mediated by PbrCSLD5, a cellulose synthase-like protein, results in cessation of pollen tube growth in Pyrus bretschneideri. Physiol Plant. 2022:**174:** e13700. https://doi.org/10.1111/ppl.13700

Lipka V, Kwon C, Panstruga R. SNARE-ware: the role of SNARE-domain proteins in plant biology. Annu Rev Cell Dev Biol. 2007:**23:** 147-174. https://doi.org/10.1146/annurev.cellbio.23.090506.123529

Lovy-Wheeler A, Cárdenas L, Kunkel J, Hepler P. Differential organelle movement on the actin cytoskeleton in lily pollen tubes. Cell Motil Cytoskeleton. 2007:**64:** 217-232. https://doi.org/10.1002/cm.20181

Mistry J, Chuguransky S, Williams L, Qureshi M, Salazar G, Sonnhammer E, Tosatto S, Paladin L, Raj S, Richardson L, et al. Pfam: The protein families database in 2021. Nucleic Acids Res. 2021:**49:** D412-D419. https://doi.org/10.1093/nar/gkaa913

Pan Q, Cui B, Deng F, Quan J, Loake G, Shan W. RTP1 encodes a novel endoplasmic reticulum (ER)-localized protein in Arabidopsis and negatively regulates resistance against biotrophic pathogens. New Phytol. 2016:**209:** 1641-1654. https://doi.org/10.1111/nph.13707

Parton R, Fischer-Parton S, Watahiki M, Trewavas A. Dynamics of the apical vesicle accumulation and the rate of growth are related in individual pollen tubes. J Cell Sci. 2001:**114:** 2685-2695. https://doi.org/10.1242/jcs.114.14.2685

Qi Z, Liu M, Dong Y, Zhu Q, Li L, Li B, Yang J, Li Y, Ru Y, Zhang H, et al. The syntaxin protein (MoSyn8) mediates intracellular trafficking to regulate conidiogenesis and pathogenicity of rice blast fungus. New Phytol. 2016:**209:** 1655-1667. https://doi.org/10.1111/nph.13710

Ruan H, Li J, Wang T, Ren H. Secretory Vesicles Targeted to Plasma Membrane During Pollen Germination and Tube Growth. Frontiers in cell and developmental biology. 2020:**8:** 615447. https://doi.org/10.3389/fcell.2020.615447

Rui Q, Tan X, Liu F, Li Y, Liu X, Li B, Wang J, Yang H, Qiao L, Li T, et al. Syntaxin of plants31 (SYP31) and SYP32 is essential for Golgi morphology maintenance and pollen development. Plant Physiol. 2021:**186:** 330-343.https://doi.org/10.1093/plphys/kiab049

Sanderfoot A, Assaad F, Raikhel N. The *Arabidopsis* genome. An abundance of soluble N-ethylmaleimide-sensitive factor adaptor protein receptors. Plant Physiol. 2000:**124:** 1558-1569. https://doi.org/10.1104/pp.124.4.1558

Schwarz D, Blower M. The endoplasmic reticulum: structure, function and response to cellular signaling. Cell Mol Life Sci. 2016:**73:** 79-94. https://doi.org/10.1007/s00018-015-2052-6

Silva P, Ul-Rehman R, Rato C, Di Sansebastiano G, Malhó R. Asymmetric localization of *Arabidopsis* SYP124 syntaxin at the pollen tube apical and sub-apical zones is involved in tip growth. BMC Plant Biol. 2010:**10:**179. https://doi.org/10.1186/1471-2229-10-179

Spang A. Retrograde traffic from the Golgi to the endoplasmic reticulum. Cold Spring Harb Perspect Biol. 2013:**5.** https://doi.org/10.1101/cshperspect.a013391

Spang A, Schekman R. Reconstitution of retrograde transport from the Golgi to the ER in vitro. J Cell Biol. 1998:**143:**589-599. https://doi.org/10.1083/jcb.143.3.589

Sparkes I, Runions J, Kearns A, Hawes C. Rapid, transient expression of fluorescent fusion proteins in tobacco plants and generation of stably transformed plants. Nat Protoc. 2006:**1:** 2019-2025. 10.1038/nprot.2006.286

Steer M, Steer J. Pollen tube tip growth. New Phytol. 1989:**111:** 323-358. https://doi.org/10.1111/j.1469-8137.1989.tb00697.x

Su X, Yan X, Chen X, Guo M, Xia Y, Cao Y. Calcofluor white hypersensitive proteins contribute to stress tolerance and pathogenicity in entomopathogenic fungus, Metarhizium acridum. Pest Manag Sci 2021:**77:** 1915-1924. https://doi.org/10.1002/ps.6218

Tang C, Wang P, Zhu X, Qi K, Xie Z, Zhang H, Li X, Gao H, Gu T, Gu C, et al. Acetylation of inorganic pyrophosphatase by S-RNase signaling induces pollen tube tip swelling by repressing pectin methylesterase. Plant Cell. 2023:1;35(9)**:**3544-3565. https://doi.org/10.1093/plcell/koad162

Teng F, Wang Y, Tang B. The syntaxins. Genome Biol. 2001:**2:** REVIEWS3012. https://doi.org/10.1186/gb-2001-2-11-reviews3012

Wang H, Niu H, Zhai Y, Lu M BiPCharacterization of Genes from Pepper (*L.*) and the Role of in Response to Endoplasmic Reticulum and Multiple Abiotic Stresses. Front Plant Sci. 2017:**8:** 1122. https://doi.org/10.3389/fpls.2017.01122

Wang M, Zhang H, Zhao X, Zhou J, Qin G, Liu Y, Kou X, Zhao Z, Wu T, Zhu J, et al. SYNTAXIN OF PLANTS81 regulates root meristem activity and stem cell niche maintenance via ROS signaling. Plant Physiol.2023:**191:**1365-1382. https://doi.org/10.1093/plphys/kiac530

Wang P, Hussey P NETWORKED 3B: a novel protein in the actin cytoskeleton-endoplasmic reticulum interaction. J Exp Bot. 2017:**68:** 1441-1450. https://doi.org/10.1093/jxb/erx047

Watson R, Pessin J. Functional cooperation of two independent targeting domains in syntaxin 6 is required for its efficient localization in the trans-golgi network of 3T3L1 adipocytes. J Biol Chem. 2000:**275:** 1261-1268. https://doi.org/10.1074/jbc.275.2.1261

Watson R, Pessin J. Transmembrane domain length determines intracellular membrane compartment localization of syntaxins 3, 4, and 5. Am J Physiol Cell Physiol. 2001:**281:** C215-223. https://doi.org/10.1152/ajpcell.2001.281.1.C215

Weimbs T, Low S, Chapin S, Mostov K, Bucher P, Hofmann K. A conserved domain is present in different families of vesicular fusion proteins: a new superfamily. Proc Natl Acad Sci U S A. 1997:**94:** 3046-3051. https://doi.org/10.1073/pnas.94.7.3046

Westrate L, Lee J, Prinz W, Voeltz G. Form follows function: the importance of endoplasmic reticulum shape. Annu Rev Biochem. 2015:**84:** 791-811. https://doi.org/10.1146/annurev-biochem-072711-163501

Wu J, Wang Z, Shi Z, Zhang S, Ming R, Zhu S, Khan M, Tao S, Korban S, Wang H, et al. The genome of the pear (*Pyrus bretschneideri* Rehd.). Genome Res. 2013:**23:** 396-408. https://doi.org/10.1101/gr.144311.112

Yang X, Xu P, Xiao Y, Xiong X, Xu T. Domain requirement for the membrane trafficking and targeting of syntaxin 1A. J Biol Chem. 2006:**281:** 15457-15463. https://doi.org/10.1074/jbc.M513246200

Ye J, Coulouris G, Zaretskaya I, Cutcutache I, Rozen S, Madden T. Primer-BLAST: a tool to design target-specific primers for polymerase chain reaction. BMC Bioinformatics. 2012:**13:** 134. https://doi.org/10.1186/1471-2105-13-134

Zheng P, Obara C, Szczesna E, Nixon-Abell J, Mahalingan K, Roll-Mecak A, Lippincott-Schwartz J, Blackstone C. ER proteins decipher the tubulin code to regulate organelle distribution. Nature. 2022:**601:** 132-138. https://doi.org/10.1038/s41586-021-04204-9

Zhou H, Yin H, Chen J, Liu X, Gao Y, Wu J, Zhang S. Gene-expression profile of developing pollen tube of *Pyrus bretschneideri*. Gene Expr Patterns. 2016:**20:** 11-21. https://doi.org/10.1016/j.gep.2015.10.004

Zhou X, Zheng Y, Wang L, Li H, Guo Y, Li M, Sun M, Zhao P. SYP72 interacts with the mechanosensitive channel MSL8 to protect pollen from hypoosmotic shock during hydration. Nat Commun. 2022:**13:** 73. https://doi.org/10.1038/s41467-021-27757-9

Figure legends

Figure 1. PbrSYP71, a member of the plant SYP7 subgroup of SNARE, was expressed in pear pollen and pollen tube. A) Sequence alignment of PbrSYP71, PbrSYP72, PbrSYP73, PbrSYP74, PbrSYP75, AtSYP71, AtSYP72 and AtSYP73. The black line represents the SNARE-Qc domain and transmembrane (TM) domain. **B)** Phylogenetic relationship of pear and Arabidopsis SYP7 subgroup proteins. The tree was generated using the Maximum Likelihood method in MEGA7. **C)** Expression level of *PbrSYP71*, *PbrSYP73*, and *PbrSYP75* in pollen grain and pollen tube were determined by RT-qPCR assay. Data are mean ± SD of 3 independent biological replicates. Different letters indicate significant differences as determined by Duncan LSD test ($P < 0.05$).

Figure 2. ***PbrSYP71* is essential for pear pollen tube growth. A)** Pear pollen treated with as-ODN for 3 h. Bars = 50 μm. The experiments were repeated 3 times with similar results, and representative pictures were shown. **B)** Expression level of *PbrSYP71* in pollen tube transfected with sense oligodeoxynucleotide of *PbrSYP71* (s-ODN), and antisense oligodeoxynucleotide (as-ODN), were determined by RT-qPCR assays. **C)** The germination rate of pollen in (A). **D)** The length of pollen tube in (A). **E)** pollen tube width in (A), at least 10 pollen tubes were measured. **F)** Cellulose content of pollen tube wall was indicated using S4B dye under s-ODN and as-ODN treatments. Bars = 10 μm. The experiments were repeated 3 times with similar results, and representative pictures were shown. **G)** Fluorescence intensity of S4B at 20 μm distance from pollen tube tips along the white thread in (F). **H)** Quantitative analysis of the S4B fluorescence intensity at the apex of the pollen tube about 5 μm from the tip along black line in (F), at least 15 pollen tubes were measured.

For (B-D), data are mean ± SD of 3 independent biological replicates. For (B-E, and H), differences were identified using Student's *t*-test, significant differences ($P < 0.01$) between means are indicated by **.

Figure 3. Intracellular localization of PbrSYP71 to the endoplasmic reticulum (ER) in tobacco leaf cells. A) Vector as control and PbrSYP71-GFP proteins were transiently expressed in transformed tobacco leaf epidermal cells. Green color represents the fluorescence intensity of GFP. The nucleus was stained by DAPI as a marker, for which the fluorescence is purple. White fluorescence showed colocalization of green and purple fluorescence. Bars = 20 μm. **B)** A locally enlarged image further shows that PbrSYP71-GFP was located in the cytoplasm, with the black arrow indicating the position of the cell wall. Bar = 5 μm. **C)** A locally enlarged image further shows that the location of PbrSYP71-GFP around the nucleus, with the black arrow indicating the position of nucleus. Bar = 5 μm. **D)** The fluorescence intensity of PbrSYP71-GFP and DAPI on the section line in Figure C. Red represents DAPI, green represents PbrSYP71. **E)** Intracellular localization of PbrSYP71-GFP and ER marker (AtRTP1-mCherry). Red color represents the fluorescence intensity of mCherry. Yellow fluorescence showed colocalization of green and red fluorescence. Bars = 20 μm.

Figure 4. PbrSYP71 is essential for endoplasmic reticulum (ER) and vesicles accumulation of pear pollen tube. A) Pear pollen tube stained by ER-tracker Red treated with as-ODN for 3 h. Bars = 10 μm. **B)** Pear pollen tube stained by FM4-64 treated with as-ODN for 3 h. Bars = 10 μm. For (A and B), the experiments were repeated 3 times with similar results, and representative pictures were shown. **C)** Quantitative analysis of ER fluorescence intensity of pollen sub-apcial area at black box in (A), 7 pollen tubes were measured. **D)** Fluorescence intensity of FM4-64 at 40 μm distance from pollen tube tips along the white thread in (B). **E)** Quantitative analysis of FM4-64 fluorescence intensity of pollen apcial area at black box in (B), at least 7 pollen tubes were measured. For (C and E), differences were identified using Student's *t*-test, significant differences ($P < 0.01$) between means are indicated by **.

Figure 5. PbrSYP71 interacts with PbrActin1. A) Schematic diagram of PbrSYP71

protein demonstrating the actin-binding domain (ABD), a SNARE-Qc domain and a transmembrane domain. **B)** Alignment of the predicted actin-binding domains in PbrSYP71 protein and AtSYP73 protein. **C)** PbrSYP71 interacts with PbrActin1 in yeast two-hybrid assays. PbrActin fused to the pGADT7 vector and that of PbrSYP71 fused to the pGBDT7 vector. Growth in the medium that lacked Leu, Trp, Ade, and His indicated protein-protein interactions. **D)** LCI assay showing interaction between PbrSYP71 and PbrActin1 in vivo. Fluorescence on the leaf surface indicated protein-protein interactions. **E)** LCI assay showing interaction between PbrSYP71-ABD and PbrActin1 in vivo.

Figure 6. The distribution of PbrSYP71 depended on actin cytoskeleton. A) Schematic diagram of segments of PbrSYP71 protein demonstrating the SYP71, SYP71-TM and SYP71-N. **B)** PbrSYP71-GFP presented bundle structure in tobacco leaf epidermal cells. Bars = 10 μm. **C)** The bundle structure of PbrSYP71-GFP collapsed to cisternae network when treated with actin cytoskeleton depolymerizing agent Cytochalasins B (CB). Bars = 10 μm. **D)** PbrSYP71-TM-GFP presented cisternae network. Bars = 10 μm. **E)** The cisternae structure of PbrSYP71-TM-GFP proteins was enlarged when treated with CB. Bars = 10 μm. **F)** PbrSYP71-N-GFP presented stronger bundle structure. Bars = 10 μm. **G)** The bundle structure of PbrSYP71-N-GFP collapsed to circles with randomly distributing when treated with CB. Bars = 10 μm. Green color represents the fluorescence intensity of GFP.

Figure 7. F-actin is essential for endoplasmic reticulum (ER) and vesicles accumulation of pear pollen tube. A) Pear pollen tubes were stained by ER-tracker Red and treated with actin cytoskeleton depolymerizing agent Cytochalasins B (CB). Bars = 10 μm. **B)** Pear pollen tubes were stained by FM4-64 and treated with CB. Bars = 10 μm. For (A and B), the experiments were repeated 3 times with similar results, and representative pictures were shown. **C)** Quantitative analysis of ER fluorescence intensity of pollen apcial area at black box in (A), at least 8 pollen tubes were measured. **D)** Fluorescence intensity of FM4-64 at 40 μm distance from pollen tube tips along the white thread in (B). **E)** Quantitative analysis of FM4-64 fluorescence intensity of pollen apcial area at black box in (B), at least 8 pollen tubes

were measured. For (C and E), differences were identified using Student's *t*-test, significant differences (P < 0.01) between means are indicated by **.

Figure 8. F-actin is essential for pear pollen tube growth. A) Pear pollen tubes were treated with actin cytoskeleton depolymerizing agent Cytochalasins B (CB) for 3 h. Bars=50 μm. The experiments were repeated 3 times with similar results, and representative pictures were shown. **B)** The germination rate of pollen in (A). **C)** The length of pollen tube in (A). **D)** pollen tube width in (A), 7 pollen tubes were measured. For (B and C) data are mean ± SD of three independent biological replicates. Differences were identified using Student's *t*-test, significant differences (P < 0.01) between means are indicated by ** . **E)** Cellulose content of pollen tube wall was indicated using S4B dye under CB treatments. Bars = 10 μm. The experiments were repeated 3 times with similar results, and representative pictures were shown. **F)** Fluorescence intensity of S4B at 20 μm distance from pollen tube tips along the white thread in (E). **G)** Quantitative analysis of the S4B fluorescence intensity at the apex of the pollen tube about 5 μm from the tip along black line in (E), at least 14 pollen tubes were measured. For (B, C, and G), differences were identified using Student's *t*-test, significant differences (P < 0.01) between means are indicated by **.

Figure 9. Hypothetical model of function of PbrSYP71 in endoplasmic reticulum (ER) distribution. A) PbrSYP71 anchors the ER to actin filament (F-actin) to maintain the accumulation of the ER at subapcial area in pear pollen tube. **B)** The accumulation of the ER was disturbed when the *PbrSYP71* expression was knocked down. **C)** The accumulation of the ER was disturbed when F-actin was depolymerized.

Figure S1. Neighbor-Joining phylogeny of SYP family proteins from *Pyrus bretschneideri* and *Arabidopsis thaliana*. The phylogenetic tree was constructed by MEGA 7.0 software using full-length protein sequences. A bootstrap analysis was conducted with 1000 replicates. Different subgroups are distinguished by different color backgrounds (SYP1-SYP8), respectively. AtSYPs and PbrSYPs from *Arabidopsis* and *Pyrus*, respectively. The scale bar is 0.1.

Figure S2. Conservative domains analysis of proteins of SYP7 subgroup. A)

Schematic diagram of SYP7 subgroup proteins demonstrating a SNARE-Qc domain. **B)** Predicted actin-binding domains (ABD) and transmembrane (TM) domain have been identified in PbrSYP71-75.

Figure S3. Conserved motif analysis of SYP proteins. A) Phylogenetic tree of the PbrSYP genes. **B)** Composition and position of 9 conserved motifs of pear PbrSYP proteins indicated by different color blocks.

Figure S4. Expression patterns of *PbrSYP* genes in different tissues of "Dangshansuli" pear. Expression patterns of *PbrSYP* genes in 19 different tissues, including 4 seedling tissues (JSM, juvenile stem; CT, cotyledon; JLF, juvenile leaf; RT, root), flower bud (FLB), stem (SM), adult leaf (ALF), leaf bud (LFB), 6 flower organ tissues (OA, ovary, SP, sepal;; ST, stamen; SY, style; PT, petal; FLS, flower stalk), 5 fruit tissues (FTC, fruit core; FS, flesh ;FTS, fruit stalk; SD, seed; PR, pericarp). The expression levels were calculated as log2-transformed (TPM) values. white, yellow, and red indicate low, moderate, and high levels, respectively.

Figure S5. The expression of *PbrSYP* genes during 4 development stages of pear pollen, including mature pollen grains (MP), hydrated pollen grains (HP), growing pollen tubes (PT) and stopped-growth pollen tubes (SPT). Color scale represents log2-transformed (FPKM) values. The expression levels were calculated as log2-transformed (RPKM) values. white, yellow, and red indicate low, moderate, and high levels, respectively.

Figure S6. Intracellular localization of PbrSYP71-TM to the endoplasmic reticulum (ER) in tobacco leaf cells. A) Schematic diagram of PbrSYP71. **B)** Schematic diagram of PbrSYP71-TM. **C)** Intracellular localization of PbrSYP71-TM-GFP and ER marker (AtRTP1-mCherry). Red color represents the fluorescence intensity of mCherry. Yellow fluorescence showed colocalization of green and red fluorescence. Bars = 20 μm.

Figure S7. The distribution of the endoplasmic reticulum (ER) and vesicle in pear Pollen tube. A) ER-Tracker Red staining distribution in a growing pollen tube of pear. Bars = 10 μm. **B)** FM4-64 staining distribution in a growing pollen tube of pear. Bars = 10 μm. **C)** Quantification of fluorescence intensity along the white line

through the bright image in (A). **D)** Quantification of fluorescence intensity along the white line through the bright image in (B).

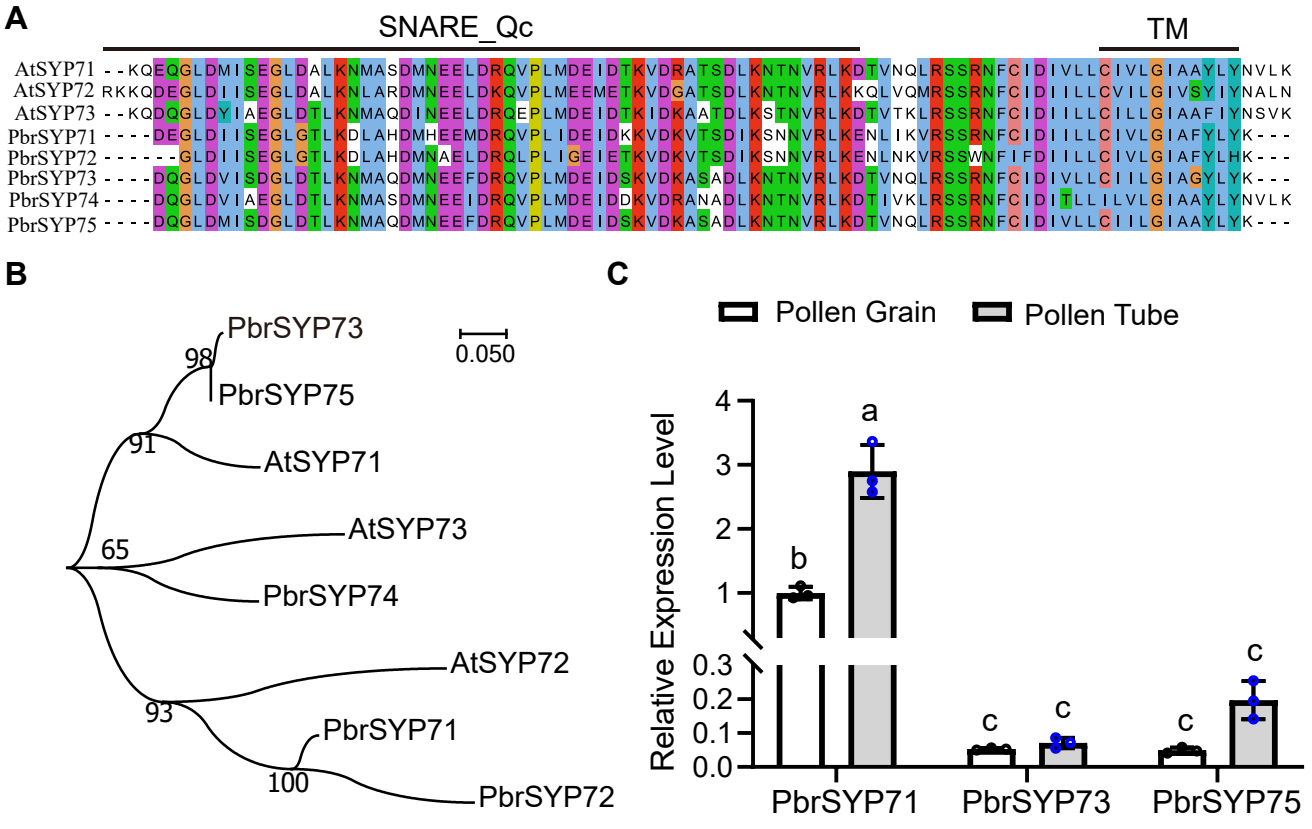

Figure 1. *PbrSYP71*, a member of the plant SYP7 subgroup of SNARE, was expressed in pear pollen and pollen tube. **A)** Sequence alignment of PbrSYP71, PbrSYP72, PbrSYP73, PbrSYP74, PbrSYP75, AtSYP71, AtSYP72 and AtSYP73. The black line represents the SNARE-Qc domain and transmembrane (TM) domain. **B)** Phylogenetic relationship of pear and Arabidopsis SYP7 subgroup proteins. The tree was generated using the Maximum Likelihood method in MEGA7. **C)** Expression level of *PbrSYP71*, *PbrSYP73*, and *PbrSYP75* in pollen grain and pollen tube were determined by RT-qPCR assay. Data are mean ± SD of 3 independent biological replicates. Different letters indicate significant differences as determined by Duncan LSD test ($P < 0.05$).

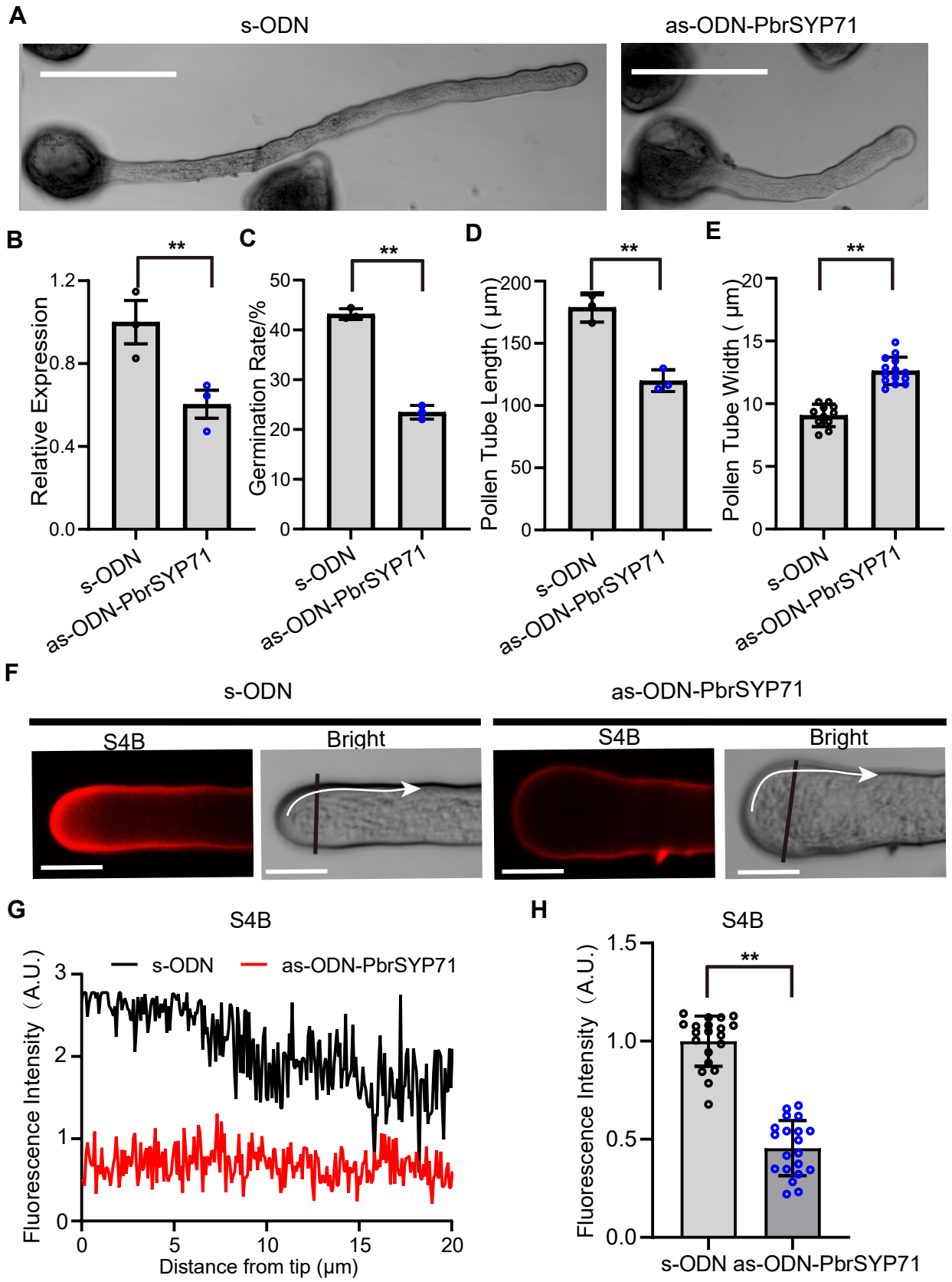

Figure 2. *PbrSYP71* is essential for pear pollen tube growth. A) Pear pollen treated with as-ODN for 3 h. Bars = 50 μm. The experiments were repeated 3 times with similar results, and representative pictures were shown. **B)** Expression level of *PbrSYP71* in pollen tube transfected with sense oligodeoxynucleotide of PbrSYP71 (s-ODN), and antisense oligodeoxynucleotide (as-ODN), were determined by RT-qPCR assays. **C)** The germination rate of pollen in (A). **D)** The length of pollen tube in (A). **E)** pollen tube width in (A), at least 10 pollen tubes were measured. **F)** Cellulose content of pollen tube wall was indicated using S4B dye under s-ODN and as-ODN treatments. Bars = 10 μm. The experiments were repeated 3 times with similar results, and representative pictures were shown. **G)** Fluorescence intensity of S4B at 20 μm distance from pollen tube tips along the white thread in (F). **H)** Quantitative analysis of the S4B fluorescence intensity at the apex of the pollen tube about 5 μm from the tip along black line in (F), at least 15 pollen tubes were measured. For (B-D), data are mean ± SD of 3 independent biological replicates. For (B-E, and H), differences were identified using Student's *t*-test, significant differences ($P < 0.01$) between means are indicated by **.

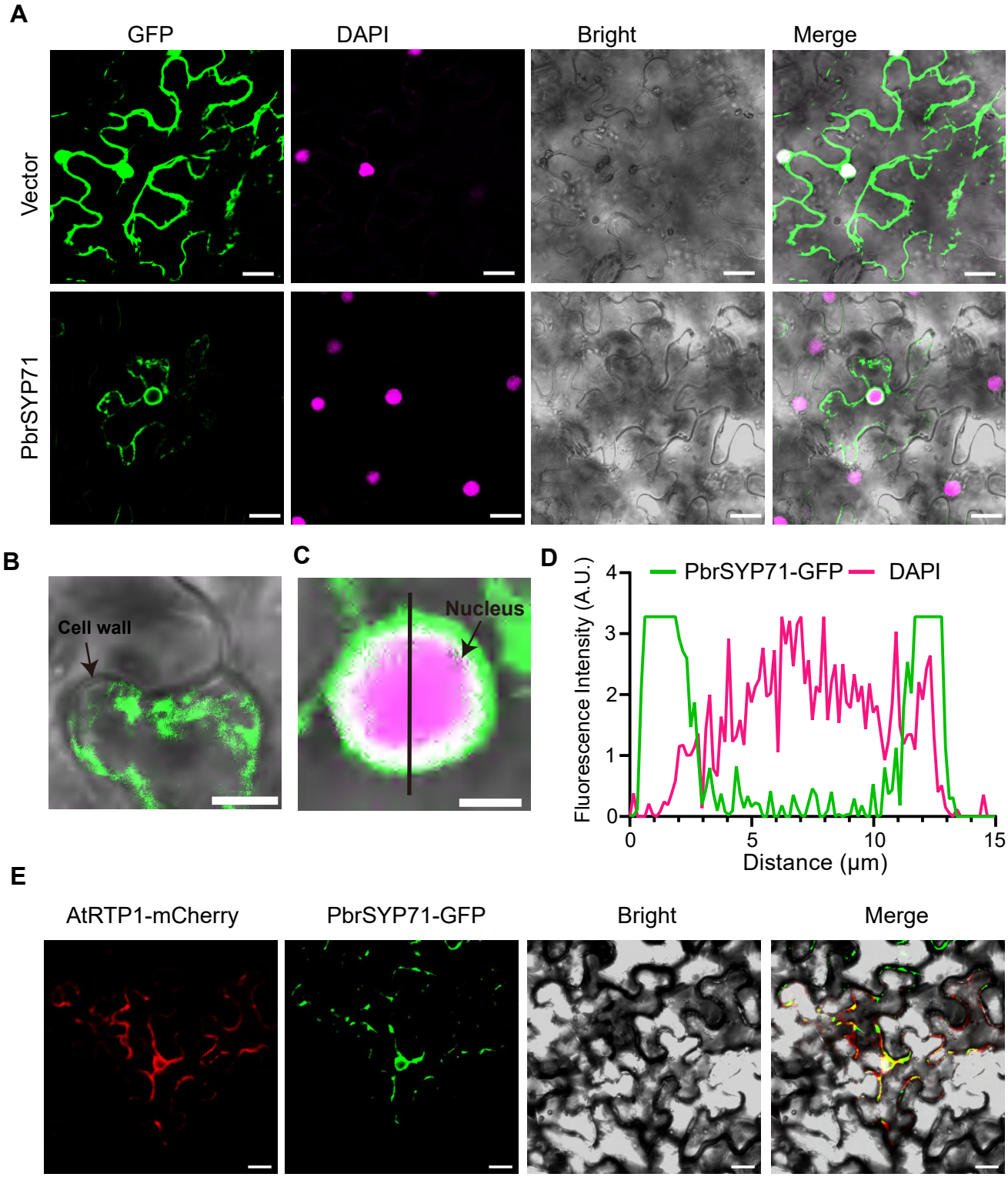

Figure 3. Intracellular localization of PbrSYP71 to the endoplasmic reticulum (ER) in tobacco leaf cells. A) Vector as control and PbrSYP71-GFP proteins were transiently expressed in transformed tobacco leaf epidermal cells. Green color represents the fluorescence intensity of GFP. The nucleus was stained by DAPI as a marker, for which the fluorescence is purple. White fluorescence showed colocalization of green and purple fluorescence. Bars = 20 μm. **B)** A locally enlarged image further shows that PbrSYP71-GFP was located in the cytoplasm, with the black arrow indicating the position of the cell wall. Bar = 5 μm. **C)** A locally enlarged image further shows that the location of PbrSYP71-GFP around the nucleus, with the black arrow indicating the position of nucleus. Bar = 5 μm. **D)** The fluorescence intensity of PbrSYP71-GFP and DAPI on the section line in Figure C. Red represents DAPI, green represents PbrSYP71. **E)** Intracellular localization of PbrSYP71-GFP and ER marker (AtRTP1-mCherry). Red color represents the fluorescence intensity of mCherry. Yellow fluorescence showed colocalization of green and red fluorescence. Bars = 20 μm.

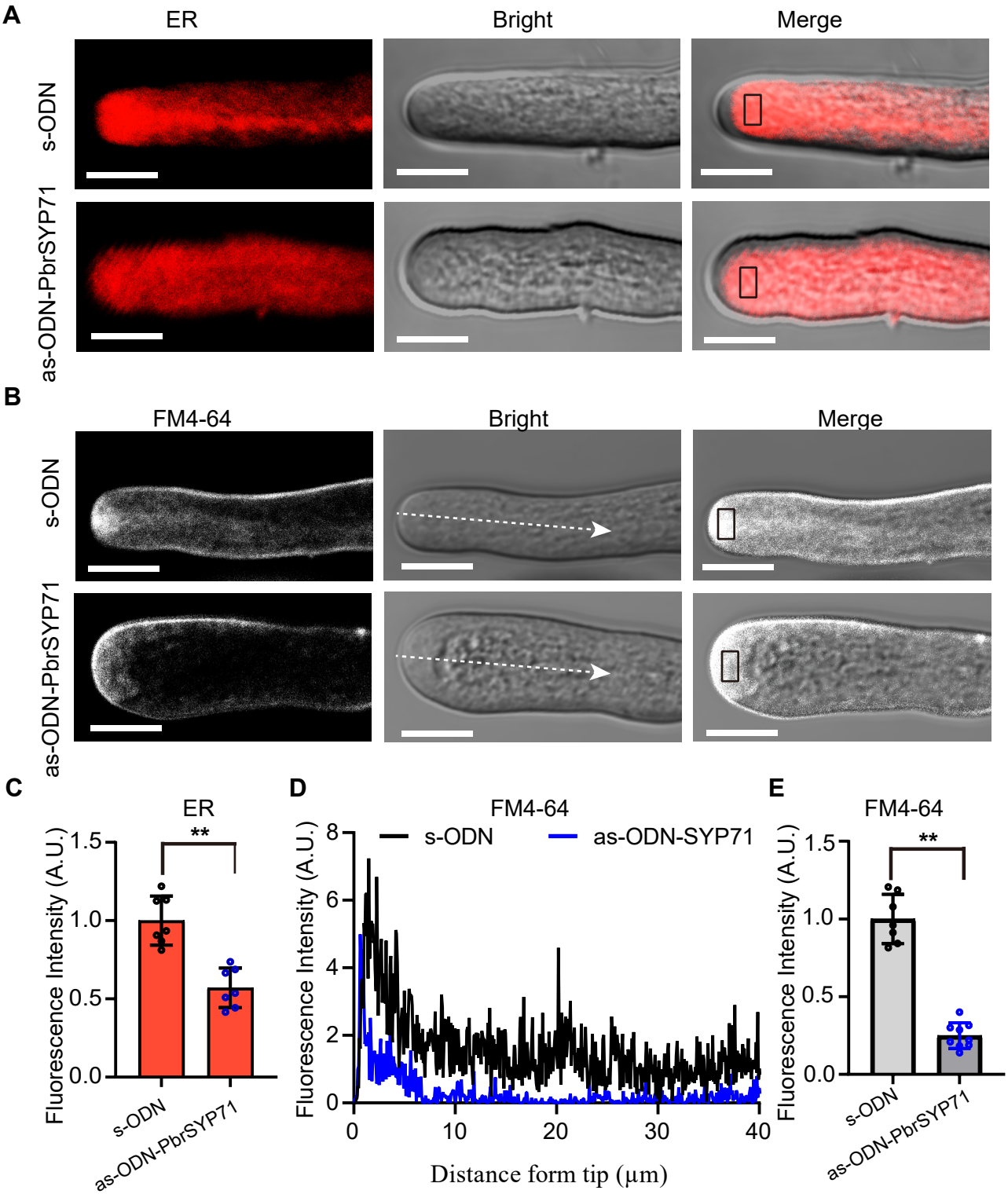

Figure 4. *PbrSYP71* is essential for endoplasmic reticulum (ER) and vesicles accumulation of pear pollen tube. A) The ER was stained with ER-tracker Red dye after treating the pollen tube with as-ODN for 3 hours. Bars = 10 μm. **B)** The vesicles were stained with FM4-64 dye after treating the pollen tube with as-ODN for 3 hours. Bars = 10 μm. For (A and B), the experiments were repeated 3 times with similar results, and representative pictures were shown. **C)** Quantitative analysis of ER fluorescence intensity of pollen sub-apcial area at black box in (A), 7 pollen tubes were measured. **D)** Fluorescence intensity of FM4-64 at 40 μm distance from pollen tube tips along the white thread in (B). **E)** Quantitative analysis of FM4-64 fluorescence intensity of pollen apcial area at black box in (B), at least 7 pollen tubes were measured. For (C and E), differences were identified using Student's *t*-test, significant differences ($P < 0.01$) between means are indicated by **.

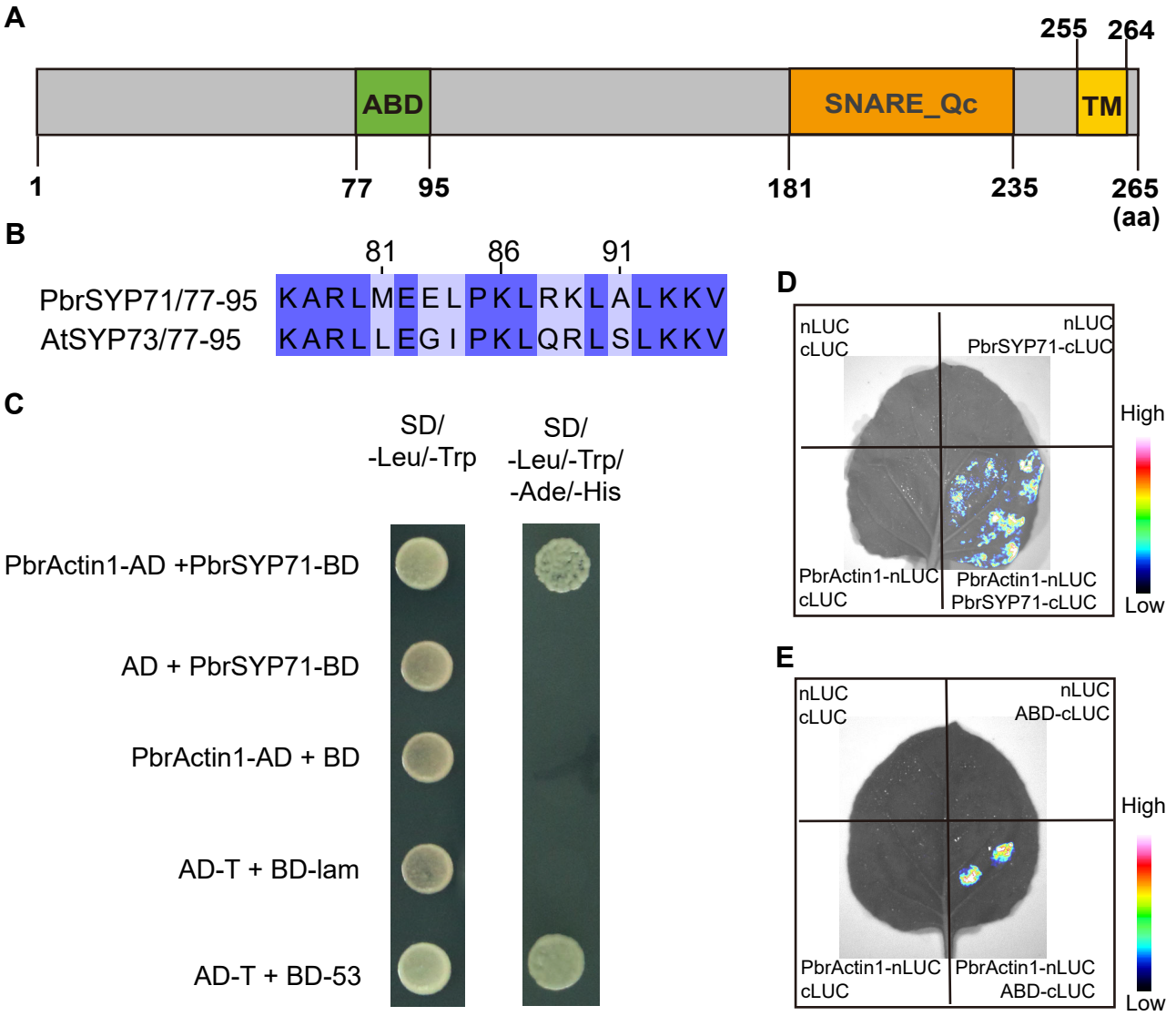

Figure 5. PbrSYP71 interacts with PbrActin1. A) Schematic diagram of PbrSYP71 protein demonstrating the actin-binding domain (ABD), a SNARE-Qc domain and a transmembrane domain (TM). **B)** Alignment of the predicted actin-binding domains in PbrSYP71 protein and AtSYP73 protein. **C)** PbrSYP71 interacts with PbrActin1 in yeast two-hybrid assays. PbrActin fused to the pGADT7 vector and that of PbrSYP71 fused to the pGBDT7 vector. Growth in the medium that lacked Leu, Trp, Ade, and His indicated protein-protein interactions. **D)** LCI assay showing interaction between PbrSYP71 and PbrActin1 in vivo. Fluorescence on the leaf surface indicated protein-protein interactions. **E)** LCI assay showing interaction between PbrSYP71-ABD and PbrActin1 in vivo.

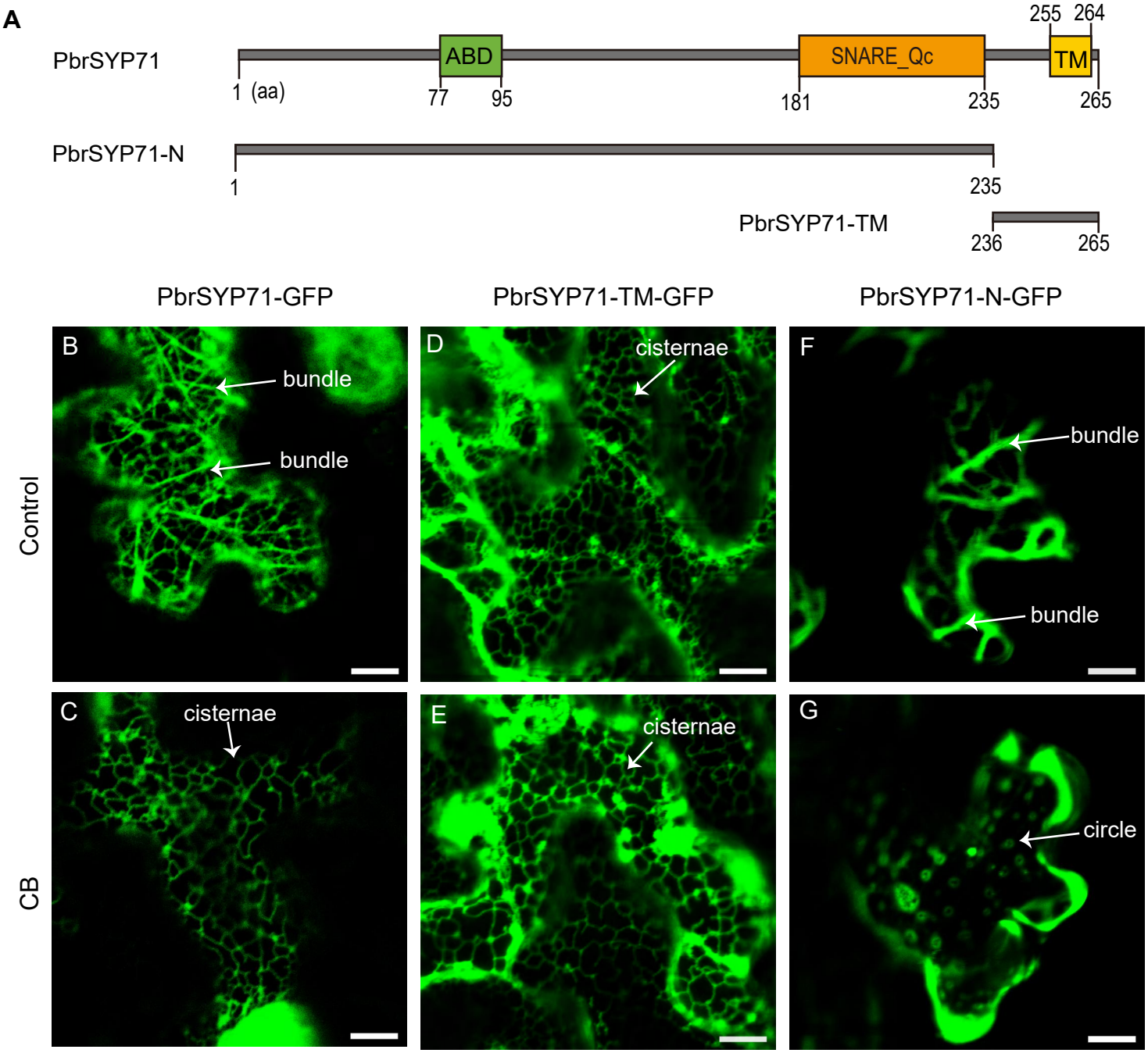

Figure 6. The distribution of PbrSYP71 depended on actin cytoskeleton. A) Schematic diagram of segments of PbrSYP71 protein demonstrating the SYP71, SYP71-TM and SYP71-N. **B)** PbrSYP71-GFP presented bundle structure in tobacco leaf epidermal cells. Bars = 10 μm. **C)** The bundle structure of PbrSYP71-GFP collapsed to cisternae network when treated with actin cytoskeleton depolymerizing agent Cytochalasins B (CB). Bars = 10 μm. **D)** PbrSYP71-TM-GFP presented cisternae network. Bars = 10 μm. **E)** The cisternae structure of PbrSYP71-TM-GFP proteins was enlarged when treated with CB. Bars = 10 μm. **F)** PbrSYP71-N-GFP presented stronger bundle structure. Bars = 10 μm. **G)** The bundle structure of PbrSYP71-N-GFP collapsed to circles with randomly distributing when treated with CB. Bars = 10 μm. Green color represents the fluorescence intensity of GFP.

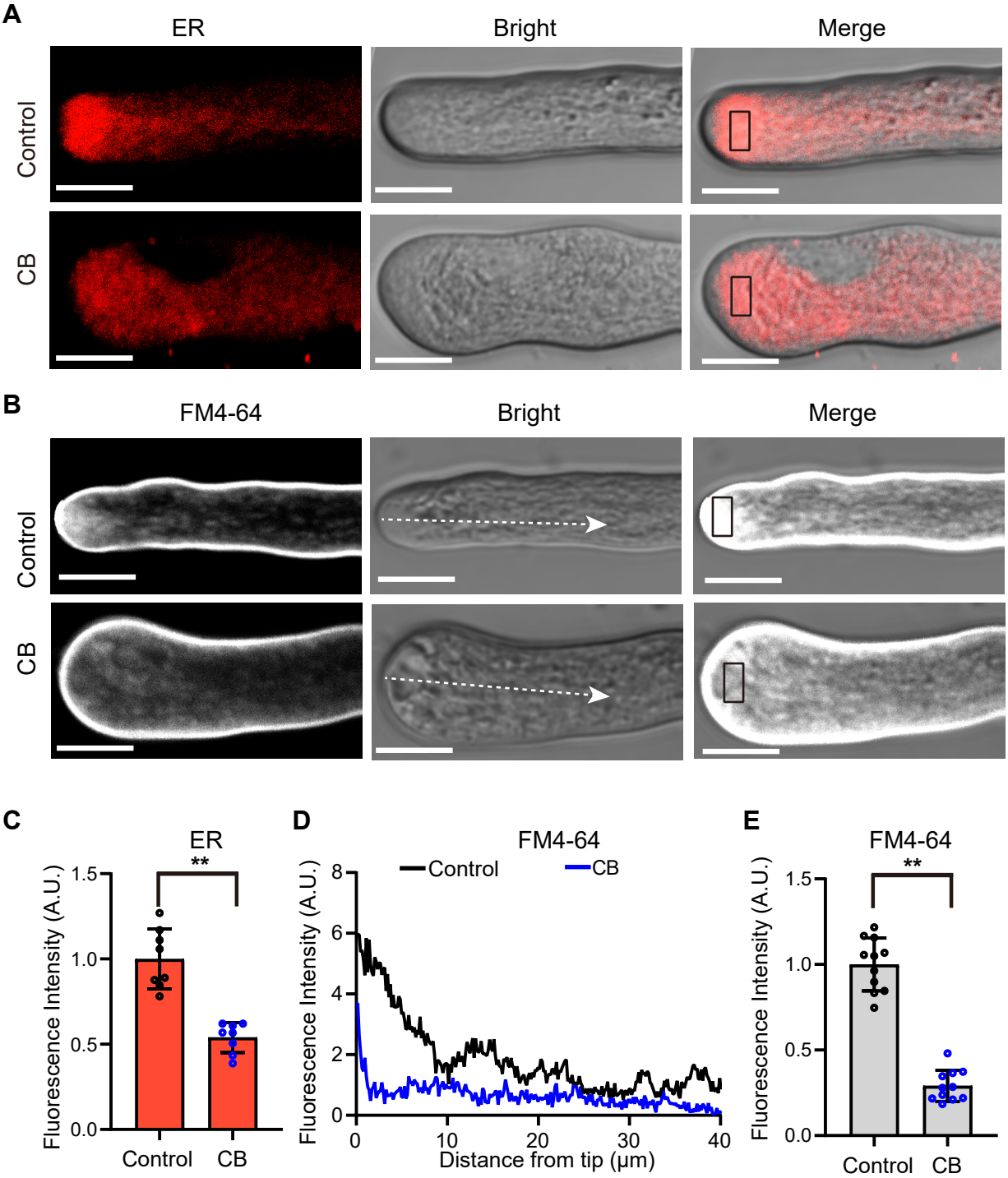

Figure 7. F-actin is essential for endoplasmic reticulum (ER) and vesicles accumulation of pear pollen tube. A) The ER was stained with ER-tracker Red dye after treating the pollen tube with actin cytoskeleton depolymerizing agent Cytochalasins B (CB). Bars = 10 μm. **B)** The vesicles were stained with FM4-64 dye after treating the pollen tube with CB. Bars = 10 μ m. For (A and B), the experiments were repeated 3 times with similar results, and representative pictures were shown. **C)** Quantitative analysis of ER fluorescence intensity of pollen apcial area at black box in (A), at least 8 pollen tubes were measured. **D)** Fluorescence intensity of FM4-64 at 40 μm distance from pollen tube tips along the white thread in (B). **E)** Quantitative analysis of FM4-64 fluorescence intensity of pollen apcial area at black box in (B), at least 8 pollen tubes were measured. For (C and E), differences were identified using Student's *t*-test, significant differences ($P < 0.01$) between means are indicated by **.

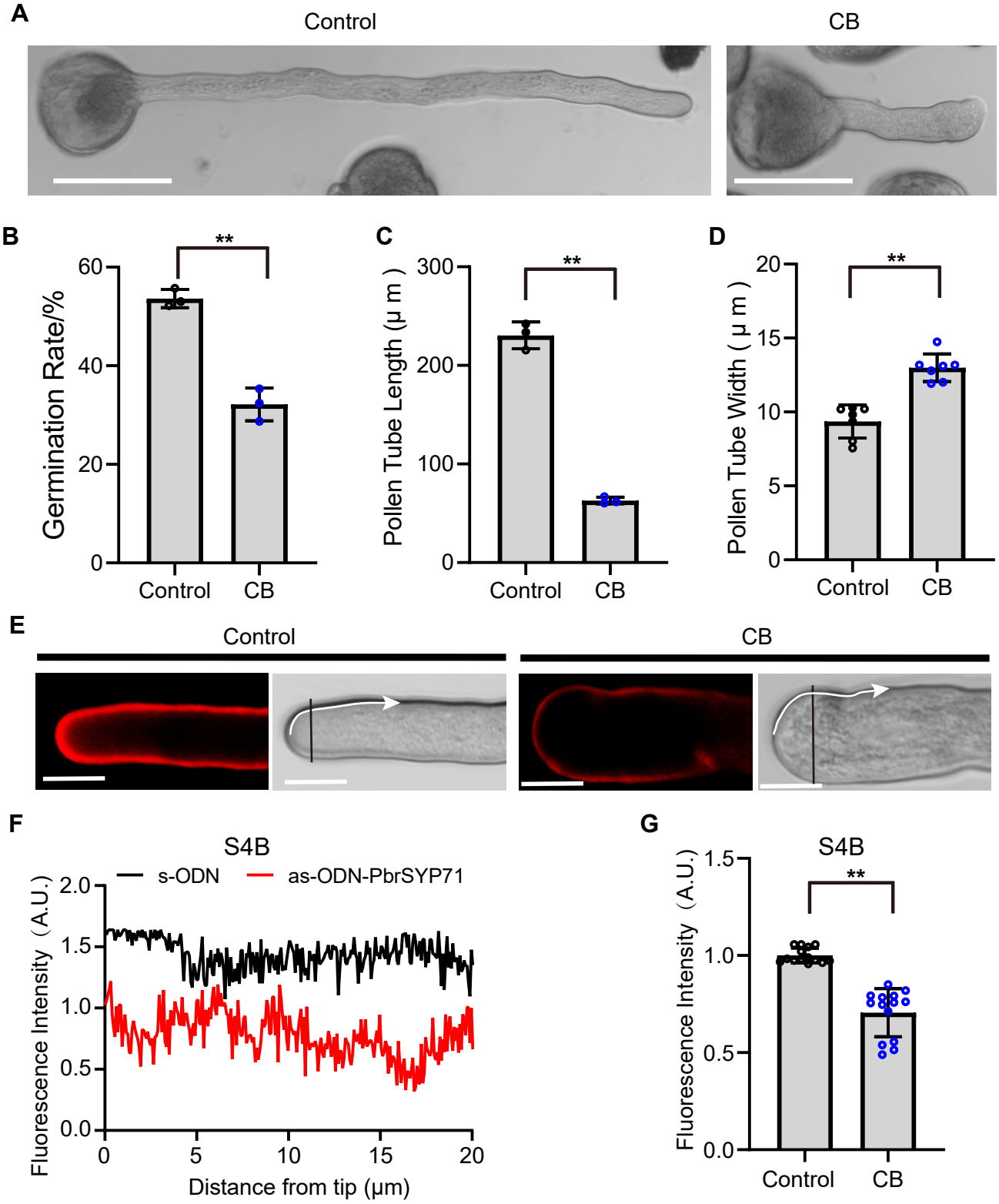

Figure 8. F-actin is essential for pear pollen tube growth. A) Pear pollen tubes were treated with actin cytoskeleton depolymerizing agent Cytochalasins B (CB) for 3 h. Bars=50 μm. The experiments were repeated 3 times with similar results, and representative pictures were shown. **B)** The germination rate of pollen in (A). **C)** The length of pollen tube in (A). **D)** pollen tube width in (A), 7 pollen tubes were measured. For (B and C) data are mean ± SD of three independent biological replicates. Differences were identified using Student's *t*-test, significant differences ($P < 0.01$) between means are indicated by ** . **E)** Cellulose content of pollen tube wall was indicated using S4B dye under CB treatments. Bars = 10 μm. The experiments were repeated 3 times with similar results, and representative pictures were shown. **F)** Fluorescence intensity of S4B at 20 μm distance from pollen tube tips along the white thread in (E). **G)** Quantitative analysis of the S4B fluorescence intensity at the apex of the pollen tube about 5 μm from the tip along black line in (E), at least 14 pollen tubes were measured. For (B, C, and G), differences were identified using Student's *t*-test, significant differences ($P < 0.01$) between means are indicated by **.

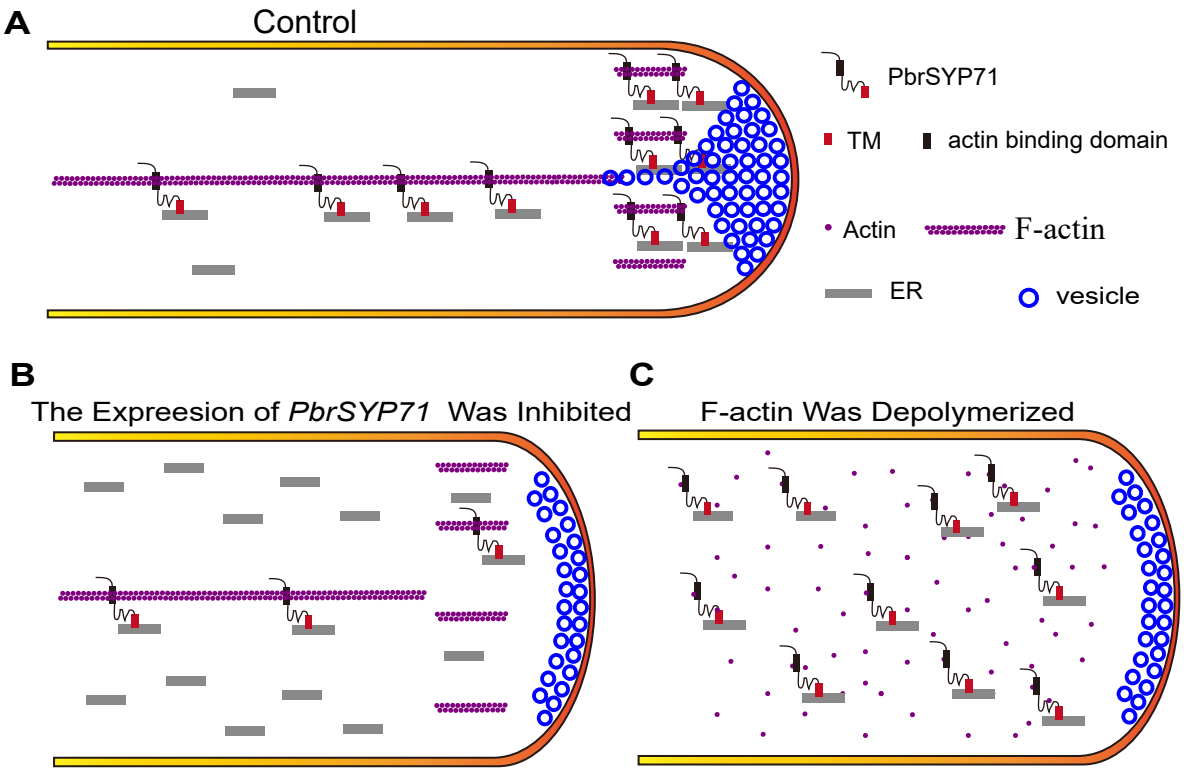

Figure 9. Hypothetical model of function of *PbrSYP71* in endoplasmic reticulum (ER) distribution. A) PbrSYP71 protein anchors the ER to actin filament (F-actin) to maintain the accumulation of the ER at subapcial area in pear pollen tube. **B)** The accumulation of the ER was disturbed when the *PbrSYP71* expression was knocked down. **C)** The accumulation of the ER was disturbed when F-actin was depolymerized.

Parsed Citations

Akita K, Kobayashi M, Sato M, Kutsuna N, Ueda T, Toyooka K, Nagata N, Hasezawa S, Higaki T. Cell wall accumulation of fluorescent proteins derived from a trans-Golgi cisternal membrane marker and paramural bodies in interdigitated Arabidopsis leaf epidermal cells. Protoplasma. 2017:254:1367-377. https://doi.org/10.1007/s00709-016-0955-1
Google Scholar: Author Only Title Only Author and Title

Artimo P, Jonnalagedda M, Arnold K, Baratin D, Csardi G, de Castro E, Duvaud S, Flegel V, Fortier A, Gasteiger E, et al. ExPASy: SIB bioinformatics resource portal. Nucleic Acids Res. 2012:40:W597-603. https://doi.org/10.1093/nar/gks400
Google Scholar: Author Only Title Only Author and Title

Bailey T, Johnson J, Grant C, Noble W. The MEME Suite. Nucleic Acids Res. 2015:43:W39-49. https://doi.org/10.1093/nar/gkv416
Google Scholar: Author Only Title Only Author and Title

Brandizzi F, Snapp E, Roberts A, Lippincott-Schwartz J, Hawes C. Membrane protein transport between the endoplasmic reticulum and the Golgi in tobacco leaves is energy dependent but cytoskeleton independent: evidence from selective photobleaching. Plant Cell. 2002:14:1293-1309. https://doi.org/10.1105/tpc.001586
Google Scholar: Author Only Title Only Author and Title

Cai G, Parrotta L, Cresti M. Organelle trafficking, the cytoskeleton, and pollen tube growth. J Integr Plant Biol. 2015:57:63-78. https://doi.org/10.1111/jipb.12289
Google Scholar: Author Only Title Only Author and Title

Campanoni P, Blatt M. Membrane trafficking and polar growth in root hairs and pollen tubes. J Exp Bot. 2007:58:65-74. https://doi.org/10.1093/jxb/erl059
Google Scholar: Author Only Title Only Author and Title

Cao P, Renna L, Stefano G, Brandizzi F. SYP73 Anchors the ER to the Actin Cytoskeleton for Maintenance of ER Integrity and Streaming in Arabidopsis. Curr Biol. 2016:26:3245-3254. https://doi.org/10.1016/j.cub.2016.10.024
Google Scholar: Author Only Title Only Author and Title

Chen C, Wu Y, Li J, Wang X, Zeng Z, Xu J, Liu Y, Feng J, Chen H, He Y, et al. TBtools-II: A "one for all, all for one" bioinformatics platform for biological big-data mining. Mol Plant. 2023:16:1733-1742. https://doi.org/10.1016/j.molp.2023.09.010
Google Scholar: Author Only Title Only Author and Title

Chen J, Wang P, de Graaf B, Zhang H, Jiao H, Tang C, Zhang S, Wu J. Phosphatidic Acid Counteracts S-RNase Signaling in Pollen by Stabilizing the Actin Cytoskeleton. Plant Cell. 2018:30:1023-1039. https://doi.org/10.1105/tpc.18.00021
Google Scholar: Author Only Title Only Author and Title

Cheung A, Wu H. Structural and functional compartmentalization in pollen tubes. J Exp Bot. 2007: 58: 75-82. https://doi.org/10.1093/jxb/erl122
Google Scholar: Author Only Title Only Author and Title

Dinkel H, Van Roey K, Michael S, Kumar M, Uyar B, Altenberg B, Milchevskaya V, Schneider M, Kühn H, Behrendt A, et al. ELM 2016--data update and new functionality of the eukaryotic linear motif resource. Nucleic Acids Res. 2016:44:D294-300. https://doi.org/10.1093/nar/gkv1291
Google Scholar: Author Only Title Only Author and Title

Dobson L, Reményi I, Tusnády G. CCTOP: a Consensus Constrained TOPology prediction web server. Nucleic Acids Res. 2015:43:W408-412. https://doi.org/10.1093/nar/gkv451
Google Scholar: Author Only Title Only Author and Title

Fan J, Yang X, Lu J, Chen L, Xu P. Role of H(abc) domain in membrane trafficking and targeting of syntaxin 1A. Biochem Biophys Res Commun. 2007:359: 245-250. https://doi.org/10.1016/j.bbrc.2007.05.065
Google Scholar: Author Only Title Only Author and Title

Gao G, Banfield D. Multiple features within the syntaxin Sed5p mediate its Golgi localization. Traffic. 202021:274-296. https://doi.org/10.1111/tra.12720
Google Scholar: Author Only Title Only Author and Title

Gupta G, Free S, Levina N, Keränen S, Heath I. Two divergent plasma membrane syntaxin-like SNAREs, nsyn1 and nsyn2, contribute to hyphal tip growth and other developmental processes in Neurospora crassa. Fungal Genet Biol. 2003:40:271-286. https://doi.org/10.1016/s1087-1845(03)00109-9
Google Scholar: Author Only Title Only Author and Title

Han J, Pluhackova K, Böckmann R. The Multifaceted Role of SNARE Proteins in Membrane Fusion. Front Physiol. 2017:8:5. https://doi.org/10.3389/fphys.2017.00005
Google Scholar: Author Only Title Only Author and Title

Hatsuzawa K, Tamura T, Hashimoto H, Hashimoto H, Yokoya S, Miura M, Nagaya H, Wada I. Involvement of syntaxin 18, an

endoplasmic reticulum (ER)-localized SNARE protein, in ER-mediated phagocytosis. Mol Biol Cell. 2006:17: 3964-3977. https://doi.org/10.1091/mbc.e05-12-1174
Google Scholar: Author Only Title Only Author and Title

Hepler P, Winship L. The pollen tube clear zone: clues to the mechanism of polarized growth. J Integr Plant Biol. 2015:57: 79-92. https://doi.org/10.1111/jipb.12315
Google Scholar: Author Only Title Only Author and Title

Hirano T, Ebine K, Ueda T, Higaki T, Watanabe-Nakayama T, Konno H, Takigawa-Imamura H, Sato M. The SYP123-VAMP727 SNARE complex delivers secondary cell wall components for root hair shank hardening in Arabidopsis. Plant Cell. 2023:30;35(12):4347-4365. https://doi.org/10.1093/plcell/koad240
Google Scholar: Author Only Title Only Author and Title

Holthuis J, Nichols B, Pelham H. The syntaxin Tlg1p mediates trafficking of chitin synthase III to polarized growth sites in yeast. Mol Biol Cell. 1998:9: 3383-3397. https://doi.org/10.1091/mbc.9.12.3383
Google Scholar: Author Only Title Only Author and Title

Hong SY, So J, Lee J, Min K, Son H, Park C, Yun SH, Lee YW. Functional analyses of two syntaxin-like SNARE genes, GzSYN1 and GzSYN2, in the ascomycete Gibberella zeae. Fungal Genet Biol. 2010:47: 364-372. https://doi.org/10.1016/j.fgb.2010.01.005
Google Scholar: Author Only Title Only Author and Title

Hu J, Huang B, Yin H, Qi K, Jia Y, Xie Z, Gao Y, Li H, Li Q, Wang Z, et al. PearMODB: a multiomics database for pear (Pyrus) genomics, genetics and breeding study. Database (Oxford). 2023:baad050. https://doi.org/10.1093/database/baad050
Google Scholar: Author Only Title Only Author and Title

Ichikawa M, Iwano M, Sato M. Nuclear membrane localization during pollen development and apex-focused polarity establishment of SYP124/125 during pollen germination in Arabidopsis thaliana. Plant Reprod. 2015:28: 143-151. https://doi.org/10.1007/s00497-015-0265-3
Google Scholar: Author Only Title Only Author and Title

Jahn R, Scheller R. SNAREs--engines for membrane fusion. Nature reviews. Nat Rev Mol Cell Biol. 2006:7: 631-643. https://doi.org/10.1038/nrm2002
Google Scholar: Author Only Title Only Author and Title

Johnson L, Eddy S, Portugaly E. Hidden Markov model speed heuristic and iterative HMM search procedure. BMC Bioinformatics. 2010:11: 431.https://doi.org/10.1186/1471-2105-11-431
Google Scholar: Author Only Title Only Author and Title

Kasai K, Akagawa K. Roles of the cytoplasmic and transmembrane domains of syntaxins in intracellular localization and trafficking. J Cell Sci. 2001:114: 3115-3124. https://doi.org/10.1242/jcs.114.17.3115
Google Scholar: Author Only Title Only Author and Title

Kawabata M, Matsuo H, Koito T, Murata M, Kubori T, Nagai H, Tagaya M, Arasaki K. Legionella hijacks the host Golgi-to-ER retrograde pathway for the association of Legionella-containing vacuole with the ER. PLoS Pathog. 2021:17: e1009437. https://doi.org/10.1371/journal.ppat.1009437
Google Scholar: Author Only Title Only Author and Title

Kumar S, Stecher G, Tamura K. MEGA7: Molecular Evolutionary Genetics Analysis Version 7.0 for Bigger Datasets. Mol Biol Evol. 2016:33: 1870-1874. https://doi.org/10.1093/molbev/msw054
Google Scholar: Author Only Title Only Author and Title

Li B, Li Y, Liu F, Tan X, Rui Q, Tong Y, Qiao L, Gao R, Li G, et al. Overexpressed Tomosyn Binds Syntaxins and Blocks Secretion during Pollen Development. Plant Physiol. 2019:181:1114-1126. https://doi.org/10.1104/pp.19.00965
Google Scholar: Author Only Title Only Author and Title

Letunic I, Khedkar S, Bork P. SMART: recent updates, new developments and status in 2020. Nucleic Acids Res. 2021:49: D458-D460. https://doi.org/10.1093/nar/gkaa937
Google Scholar: Author Only Title Only Author and Title

Li X, Tang C, Li X, Zhu X, Cai Y, Wang P, Zhang S, Wu J. Cellulose accumulation mediated by PbrCSLD5, a cellulose synthase-like protein, results in cessation of pollen tube growth in Pyrus bretschneideri. Physiol Plant. 2022:174: e13700. https://doi.org/10.1111/ppl.13700
Google Scholar: Author Only Title Only Author and Title

Lipka V, Kwon C, Panstruga R. SNARE-ware: the role of SNARE-domain proteins in plant biology. Annu Rev Cell Dev Biol. 2007:23: 147-174. https://doi.org/10.1146/annurev.cellbio.23.090506.123529
Google Scholar: Author Only Title Only Author and Title

Lovy-Wheeler A, Cárdenas L, Kunkel J, Hepler P. Differential organelle movement on the actin cytoskeleton in lily pollen tubes. Cell Motil Cytoskeleton. 2007:64: 217-232. https://doi.org/10.1002/cm.20181

Google Scholar: Author Only Title Only Author and Title

Mistry J, Chuguransky S, Williams L, Qureshi M, Salazar G, Sonnhammer E, Tosatto S, Paladin L, Raj S, Richardson L, et al. Pfam: The protein families database in 2021. Nucleic Acids Res. 2021:49: D412-D419. https://doi.org/10.1093/nar/gkaa913
Google Scholar: Author Only Title Only Author and Title

Pan Q, Cui B, Deng F, Quan J, Loake G, Shan W. RTP1 encodes a novel endoplasmic reticulum (ER)-localized protein in Arabidopsis and negatively regulates resistance against biotrophic pathogens. New Phytol. 2016:209: 1641-1654. https://doi.org/10.1111/nph.13707
Google Scholar: Author Only Title Only Author and Title

Parton R, Fischer-Parton S, Watahiki M, Trewavas A. Dynamics of the apical vesicle accumulation and the rate of growth are related in individual pollen tubes. J Cell Sci. 2001:114: 2685-2695. https://doi.org/10.1242/jcs.114.14.2685
Google Scholar: Author Only Title Only Author and Title

Qi Z, Liu M, Dong Y, Zhu Q, Li L, Li B, Yang J, Li Y, Ru Y, Zhang H, et al. The syntaxin protein (MoSyn8) mediates intracellular trafficking to regulate conidiogenesis and pathogenicity of rice blast fungus. New Phytol. 2016:209: 1655-1667. https://doi.org/10.1111/nph.13710
Google Scholar: Author Only Title Only Author and Title

Ruan H, Li J, Wang T, Ren H. Secretory Vesicles Targeted to Plasma Membrane During Pollen Germination and Tube Growth. Frontiers in cell and developmental biology. 2020:8: 615447. https://doi.org/10.3389/fcell.2020.615447
Google Scholar: Author Only Title Only Author and Title

Rui Q, Tan X, Liu F, Li Y, Liu X, Li B, Wang J, Yang H, Qiao L, Li T, et al. Syntaxin of plants31 (SYP31) and SYP32 is essential for Golgi morphology maintenance and pollen development. Plant Physiol. 2021:186: 330-343.https://doi.org/10.1093/plphys/kiab049
Google Scholar: Author Only Title Only Author and Title

Sanderfoot A, Assaad F, Raikhel N. The Arabidopsis genome. An abundance of soluble N-ethylmaleimide-sensitive factor adaptor protein receptors. Plant Physiol. 2000:124: 1558-1569. https://doi.org/10.1104/pp.124.4.1558
Google Scholar: Author Only Title Only Author and Title

Schwarz D, Blower M. The endoplasmic reticulum: structure, function and response to cellular signaling. Cell Mol Life Sci. 2016:73: 79-94. https://doi.org/10.1007/s00018-015-2052-6
Google Scholar: Author Only Title Only Author and Title

Silva P, Ul-Rehman R, Rato C, Di Sansebastiano G, Malhó R. Asymmetric localization of Arabidopsis SYP124 syntaxin at the pollen tube apical and sub-apical zones is involved in tip growth. BMC Plant Biol. 2010:10:179. https://doi.org/10.1186/1471-2229-10-179
Google Scholar: Author Only Title Only Author and Title

Spang A. Retrograde traffic from the Golgi to the endoplasmic reticulum. Cold Spring Harb Perspect Biol. 2013:5. https://doi.org/10.1101/cshperspect.a013391
Google Scholar: Author Only Title Only Author and Title

Spang A, Schekman R. Reconstitution of retrograde transport from the Golgi to the ER in vitro. J Cell Biol. 1998:143:589-599. https://doi.org/10.1083/jcb.143.3.589
Google Scholar: Author Only Title Only Author and Title

Sparkes I, Runions J, Kearns A, Hawes C. Rapid, transient expression of fluorescent fusion proteins in tobacco plants and generation of stably transformed plants. Nat Protoc. 2006:1: 2019-2025. 10.1038/nprot.2006.286
Google Scholar: Author Only Title Only Author and Title

Steer M, Steer J. Pollen tube tip growth. New Phytol. 1989:111: 323-358. https://doi.org/10.1111/j.1469-8137.1989.tb00697.x
Google Scholar: Author Only Title Only Author and Title

Su X, Yan X, Chen X, Guo M, Xia Y, Cao Y. Calcofluor white hypersensitive proteins contribute to stress tolerance and pathogenicity in entomopathogenic fungus, Metarhizium acridum. Pest Manag Sci 2021:77: 1915-1924. https://doi.org/10.1002/ps.6218
Google Scholar: Author Only Title Only Author and Title

Tang C, Wang P, Zhu X, Qi K, Xie Z, Zhang H, Li X, Gao H, Gu T, Gu C, et al. Acetylation of inorganic pyrophosphatase by S-RNase signaling induces pollen tube tip swelling by repressing pectin methylesterase. Plant Cell. 2023:1;35(9):3544-3565. https://doi.org/10.1093/plcell/koad162
Google Scholar: Author Only Title Only Author and Title

Teng F, Wang Y, Tang B. The syntaxins. Genome Biol. 2001:2: REVIEWS3012. https://doi.org/10.1186/gb-2001-2-11-reviews3012
Google Scholar: Author Only Title Only Author and Title

Wang H, Niu H, Zhai Y, Lu M BiPCharacterization of Genes from Pepper (L.) and the Role of in Response to Endoplasmic Reticulum and Multiple Abiotic Stresses. Front Plant Sci. 2017:8: 1122. https://doi.org/10.3389/fpls.2017.01122
Google Scholar: Author Only Title Only Author and Title

Wang M, Zhang H, Zhao X, Zhou J, Qin G, Liu Y, Kou X, Zhao Z, Wu T, Zhu J, et al. SYNTAXIN OF PLANTS81 regulates root meristem activity and stem cell niche maintenance via ROS signaling. Plant Physiol.2023:191:1365-1382. https://doi.org/10.1093/plphys/kiac530
Google Scholar: Author Only Title Only Author and Title

Wang P, Hussey P NETWORKED 3B: a novel protein in the actin cytoskeleton-endoplasmic reticulum interaction. J Exp Bot. 2017:68: 1441-1450. https://doi.org/10.1093/jxb/erx047
Google Scholar: Author Only Title Only Author and Title

Watson R, Pessin J. Functional cooperation of two independent targeting domains in syntaxin 6 is required for its efficient localization in the trans-golgi network of 3T3L1 adipocytes. J Biol Chem. 2000:275: 1261-1268. https://doi.org/10.1074/jbc.275.2.1261
Google Scholar: Author Only Title Only Author and Title

Watson R, Pessin J. Transmembrane domain length determines intracellular membrane compartment localization of syntaxins 3, 4, and 5. Am J Physiol Cell Physiol. 2001:281: C215-223. https://doi.org/10.1152/ajpcell.2001.281.1.C215
Google Scholar: Author Only Title Only Author and Title

Weimbs T, Low S, Chapin S, Mostov K, Bucher P, Hofmann K. A conserved domain is present in different families of vesicular fusion proteins: a new superfamily. Proc Natl Acad Sci U S A. 1997:94: 3046-3051. https://doi.org/10.1073/pnas.94.7.3046
Google Scholar: Author Only Title Only Author and Title

Westrate L, Lee J, Prinz W, Voeltz G. Form follows function: the importance of endoplasmic reticulum shape. Annu Rev Biochem. 2015:84: 791-811. https://doi.org/10.1146/annurev-biochem-072711-163501
Google Scholar: Author Only Title Only Author and Title

Wu J, Wang Z, Shi Z, Zhang S, Ming R, Zhu S, Khan M, Tao S, Korban S, Wang H, et al. The genome of the pear (Pyrus bretschneideri Rehd.). Genome Res. 2013:23: 396-408. https://doi.org/10.1101/gr.144311.112
Google Scholar: Author Only Title Only Author and Title

Yang X, Xu P, Xiao Y, Xiong X, Xu T. Domain requirement for the membrane trafficking and targeting of syntaxin 1A. J Biol Chem. 2006:281: 15457-15463. https://doi.org/10.1074/jbc.M513246200
Google Scholar: Author Only Title Only Author and Title

Ye J, Coulouris G, Zaretskaya I, Cutcutache I, Rozen S, Madden T. Primer-BLAST: a tool to design target-specific primers for polymerase chain reaction. BMC Bioinformatics. 2012:13: 134. https://doi.org/10.1186/1471-2105-13-134
Google Scholar: Author Only Title Only Author and Title

Zheng P, Obara C, Szczesna E, Nixon-Abell J, Mahalingan K, Roll-Mecak A, Lippincott-Schwartz J, Blackstone C. ER proteins decipher the tubulin code to regulate organelle distribution. Nature. 2022:601: 132-138. https://doi.org/10.1038/s41586-021-04204-9
Google Scholar: Author Only Title Only Author and Title

Zhou H, Yin H, Chen J, Liu X, Gao Y, Wu J, Zhang S. Gene-expression profile of developing pollen tube of Pyrus bretschneideri. Gene Expr Patterns. 2016:20: 11-21. https://doi.org/10.1016/j.gep.2015.10.004
Google Scholar: Author Only Title Only Author and Title

Zhou X, Zheng Y, Wang L, Li H, Guo Y, Li M, Sun M, Zhao P. SYP72 interacts with the mechanosensitive channel MSL8 to protect pollen from hypoosmotic shock during hydration. Nat Commun. 2022:13: 73. https://doi.org/10.1038/s41467-021-27757-9
Google Scholar: Author Only Title Only Author and Title